EQUILIBRIUM MOISTURE CONTENT MEASUREMENT FOR POROUS BUILDING MATERIALS AT VARIOUS TEMPERATURES

by

Joseph Richard Edwards

Thesis submitted to the Faculty of the

Virginia Polytechnic Institute and State University

in partial fulfillment of the requirements for the degree of

MASTER OF SCIENCE
in
MECHANICAL ENGINEERING

APPROVED:

William C. Thomas
Dr. William C. Thomas, Chairman

F J Pierce
Dr. Felix J. Pierce

Elaine P. Scott
Dr. Elaine P. Scott

May, 1996
Blacksburg, VA

c. 2

LD
5655
V855
1996
E393
c.2

EQUILIBRIUM MOISTURE CONTENT MEASUREMENT FOR POROUS BUILDING MATERIALS AT VARIOUS TEMPERATURES

by
Joseph Richard Edwards

Dr. William C. Thomas, Chairman
Mechanical Engineering

(ABSTRACT)

Sorption isotherms and scanning data were obtained for three test materials at three different temperatures. These data resulted from further investigating the operating range of an existing experimental apparatus and procedure. During the course of the research, the operating range and control of the existing apparatus were extended, and its temperature range was tested for the first time.

The apparatus is composed of a small test chamber, which is capable of containing from one to six test samples, and an external forced-air relative humidity and temperature conditioning system. The conditioning system maintains test chamber relative humidity and temperature, as directed by a GW-BASIC computer program. Sample moisture content is gravimetrically determined in situ. The system can maintain dry-bulb temperatures between 10 C and 70 C. At room temperature, the apparatus can maintain relative humidities between 0 and 90 per cent. Low temperature set points have a significantly lower maximum relative humidity range as a result of the formation of condensation in the concentric tube counterflow heat exchanger. High temperature set points are also severely limited, due to

the formation of condensation in the test chamber during data collection.

Sorption isotherms were measured for oriented strand board, fiber board sheathing, and exterior grade plywood over the relative humidity range limits at 12 C, 25 C, and 55 C. Scanning curves were measured from the 50 per cent relative humidity set points on the adsorption and desorption curves of the 25 C isotherms.

ACKNOWLEDGEMENTS

I would like to thank my advisor, Dr. W.C. Thomas, for his support, guidance, and, most importantly, his patience as I struggled to master the "experimental method." I would also like to thank my committee members, Dr. F.J. Pierce and Dr. E.P. Scott.

I would like to thank my parents, Charles and Jean Edwards, for their love and support for the past 24 years.

I respectfully acknowledge NIST for supporting this research financially.

Many thanks also go to Justin Nave, Tim Conway, John "The Cool Bro" Scott, Andrew Edwards, Joy Corson, Brandon "Bol" Scott, and Robert Piccoli, for helping me keep my work in perspective.

I would also like to thank the people who made my lab a nice place to work - Vincent Chevrier, John Risi, and Hume Peabody.

To my personal heroes George Probst, Steve Taylor, Jeremy Koren, and Matt Zacharias, I thank you for setting the standards for which I strive.

I would also like to thank Mike Cox and Wes Schilling for everything that they have done for me.

TABLE OF CONTENTS

INTRODUCTION 1
Motivation for the Research 1
Effect of Moisture Content on Wood 2
Moisture Content in Porous Materials 4
The Sorption Isotherm 5
Hysteresis effect 10
Scanning curves 10
Analytical and Empirical Models 11
General moisture transfer theory 13
Experimental Findings 15
Scope of the Research 16

EXPERIMENTAL APPARATUS AND PROCEDURE 17
Test Chamber 17
External Conditioning System 20
Circulation 21
Test Chamber Temperature Control 21
Temperature measurement 24
Test Chamber Relative Humidity Control 24
Bubble and desiccant tubes 26
Relative humidity measurement 26
Automated Control of Temperature and Relative Humidity 30
Control algorithm 30
Equilibrium Moisture Content 32
Mass measurement 32
Specimen containers 34
Determination of dry mass 35
Experimental Procedure 36
Test specimen preparation 37
Saturation of specimens 38
Sorption isotherm 39
Scanning curves 39

RESULTS AND DISCUSSION 41
Performance Capabilities of the Apparatus 41
Long-term control of the test chamber relative humidity and temp 43

Short-term control of the test chamber relative humidity and temp 45
Maximum test chamber relative humidity 48
Moisture Content Results 49
Discussion of sorption isotherm results 54
Analysis of scanning data 58
Analysis of the temperature effect 62
Results Summary 64
Recommendations for future research 65

CONCLUSIONS 67

REFERENCES 69

APPENDIX A 74

APPENDIX B 80

APPENDIX C 90

APPENDIX D 93

VITA 96

LIST OF FIGURES

Figure 1. Type I, II, and III sorption isotherms. 6

Figure 2. Type IV and V sorption isotherms. 6

Figure 3. Type II sorption isotherm. 7

Figure 4. Schematic diagram of the experimental apparatus. 18

Figure 5. Photograph of the experimental apparatus 18

Figure 6. Photograph of the temperature bath and circulator. 23

Figure 7. Photograph of the power supply and power supply programmer 23

Figure 8. View of Vaisala probes inserted in chamber. 27

Figure 9. Photograph of the dew point hygrometer with the two filters 29

Figure 10. Photograph of the dew point monitor. 29

Figure 11. Photograph of hook used to maneuver and weigh specimens. 33

Figure 12. Photograph of the electronic scale mounted above test chamber. 34

Figure 13. Photograph of the test chamber with six samples inside. 35

Figure 14. Schematic diagram of the apparatus configured for extreme temperatures . 43

Figure 15. Stability of test chamber relative humidity. 46

Figure 16. Stability of test chamber temperature. 46

Figure 17. System response to a step change in relative humidity from 50 to 65 % . . . 47

Figure 18. Sorption isotherm for EGS at 12 C. 50

Figure 19. Sorption isotherm for EGS at 25 C. 50

Figure 20. Sorption isotherm for EGS at 55 C. 51

Figure 21. Sorption isotherm for OSB at 12 C. 51

Figure 22. Sorption isotherm for OSB at 25 C. 52

Figure 23. Sorption isotherm for OSB at 55 C. 52

Figure 24. Sorption isotherm for FBS at 12 C. 53

Figure 25. Sorption isotherm for FBS at 25 C. 53

Figure 26. Sorption isotherm for FBS at 55 C. 54

Figure 27. Comparison of current 25 C EGS adsorption curve with existing data 57

Figure 28. Sorption isotherm with scanning curves for EGS at 25 C. 59

Figure 29. Sorption isotherm with scanning curves for OSB at 25 C. 59

Figure 30. Sorption isotherm with scanning curves for FBS at 25 C. 60

Figure 31. Comparison of Pederson's approximation with current EGS desorption-to-adsorption scanning data. 61

Figure 32. Comparison of Pederson's approximation with current EGS adsorption-to-desorption scanning data. 62

Figure 33. Variation of the average sorption isotherm of EGS with temperature 63

Figure 34. Variation of the average sorption isotherm of OSB with temperature. 63

Figure 35. Variation of the average sorption isotherm of FBS with temperature. 64

LIST OF TABLES

Table 1. Test chamber control and precision data for the current apparatus. 44

Table 2. Previous test chamber control and precision data (Peters, 1992) 44

Table A-1. Equilibrium moisture content adsorption data for all test specimens at 25 C 74

Table A-2. Equlibrium moisture content desorption data for all test specimens at 25 C 75

Table A-3. Equilibrium moisture content adsorption data for all test specimens at 12 C 76

Table A-4. Equilibrium moisture content desorption data for all test specimens at 12 C. 77

Table A-5. Equilibrium moisture content adsorption data for all test specimens at 55 C. 78

Table A-6. Equilibrium moisture content desorption data for all test specimens at 55 C. 78

Table A-7. Adsorption scanning data for all test specimens at 25 C. 79

Table A-8. Desorption scanning data for all test specimens at 25 C. 79

Table C-1. A/D ratios for the 25 C isotherms. 91

Table C-2. A/D ratios for the 12 C sorption isotherms. 92

Table C-3. A/D ratios for the 55 C sorption isotherms. 92

Table D-1. Comparison of Pederson's approximation and its revised form with the current data. 94

Table D-2. Comparison of Pederson's approximation and its revised form with the current adsorption-to-desorption scanning data. 94

Table D-3. Comparison of Pederson's approximatioon and its revised form with Peters' data 95

Table D-4. Comparison of Pederson's approximation and its revised form with Peralta's data. 95

NOMENCLATURE

SYMBOLS

c	capacity
C	concentration
D	diffusion coefficient
e	error
h	enthalpy
J	mass transferred
k	constant
m	number of steps
M	mass of sample
p	pressure
RH	relative humidity (%)
s	entropy
T	temperature
v	specific volume
x	spatial variable

GREEK SYMBOLS

γ	fractional moisture content

ρ	density
τ	constant
ϕ	humidity fraction

SUBSCRIPTS

0	initial
a	adsorption
A	identifier, i.e. "sample A"
d	desorption
D	derivative
db	dry-bulb
dp	dew point
eq	equilibrium
I	integral
l	liquid
m	mass
P	proportional
q	heat
s	sample
sat	saturation
v	vapor

INTRODUCTION

The hygroscopic nature of common building materials has inspired a great deal of research in recent years. The interest is due to the effect of moisture content upon the mechanical and dielectric properties of these materials. Reliable data are needed to establish a theoretical model of moisture absorption in porous media, which can be applied in a manner that optimizes target properties of the material in use. The purpose of this research is to extend the range and increase the stability of an experimental method which was previously used by Peters (1992).

Motivation for the Research

The motivation for the current research is the potential for the existing experimental method to provide reliable moisture content data over a wide range of humidities and temperatures. These data will aid in the development of an accurate analytical model of mass and heat transfer in porous materials. Such analytical models have been developed in recent years by Thomas and Burch (1990), Kumaran (1990), Burch

and Thomas (1991), Krus (1992), Wadsö (1994), Peralta (1995b), and Cunningham (1995). None of the available analytical models can be properly applied and, therefore, evaluated until a sufficient amount of accurate material property data are available.

The lack of such data has been pointed out in some of the literature, most notably in Thomas and Burch (1990) and Kumaran (1990). In the more recent analytical models, data were provided by the researcher for the specific purpose of the model, such as in Wadsö (1994). Peralta (1995b) used the data from Peralta (1995a) for his method. Cunningham (1995) relied upon the work of Wadsö. In order for any of these models to achieve universal credibility, an adequate amount of independently determined moisture property data must be shown to be in agreement. Improving a fast and accurate method of obtaining moisture property data is the focus of the current research.

Effect of Moisture Content on Wood

Sorption is considered important in the construction industry because of the effect of moisture content upon the mechanical and dielectric properties of wood and wood-based materials. Mechanical properties of wood are defined for wood at a moisture content of 12 per cent. However, properties can be significantly affected by deviations from this moisture content level.

For wood preservation, the general rule is that less moisture is better. A low

moisture content is ideal for most cases because the wood is strongest in a dry state. Other important considerations include the fact that the thermal and electrical conductivities are minimized at low moisture content, and that there is little danger of mold formation if the wood is dry. Dry wood is also a good clean energy source, producing 60 per cent of the energy of coal while leaving ash which is an effective fertilizer (Findlay, 1975).

Maintaining wood in a structure at an extremely low moisture content, however, can be dangerous because the wood will swell when exposed to ambient conditions, which can lead to warping, splitting or mechanical failure. Douglas fir, which is commonly used to make plywood, shrinks by 12 per cent when its moisture content goes from 12 per cent to 0 per cent (Findlay, 1975). An additional danger is that the board can fail as a result of its reduced mechanical properties at the higher moisture content. If the moisture content is high enough to maintain a condition at the surface which is above the mold species threshold, mold will form (International Energy Agency, 1990).

The properties of wood which are enhanced by higher moisture content are the thermal and electrical conductivities. Wood becomes a much better conductor as the air spaces in its structure are filled with water. Electrical conductivity varies so strongly with moisture content that its measurement is the most common indicator of moisture content. Along the adsorption curve, the electrical conductivity increases by 10^{10} to 10^{13} times (Forest Products Laboratory, 1974).

Moisture Content in Porous Materials

Moisture content is defined as the mass of water in the material expressed as a fraction of its dry mass, which is its mass after being oven-dried at 102 C (Forest Products Laboratory, 1974). However, drying wood at this or higher temperatures can permanently affect its mechanical and dielectric properties. In order to preserve its natural properties, the dry mass in the context of the current research will be considered the equilibrium mass of the wood sample at the test temperature and 0 per cent relative humidity. This basis provides a more reliable standard, since the effects of elevated temperature upon the wood cannot always be accurately determined.

The Forest Products Laboratory (1974) states that the short-term effects of elevated temperatures below 200° F are almost fully reversible. However, the dry mass of wood has been defined as its mass after it has been dried in an oven above the boiling point of water (Findlay, 1975). Therefore, wood which has been dried in this manner may have experienced irreversible property changes. Drying the samples as much as possible at the isotherm temperature allows the wood to maintain its natural properties.

A wood sample will achieve equilibrium with its environment by absorbing or releasing moisture, depending upon how the relative humidity of the environment is changing. There are three methods of moisture storage in wood - liquid water in the cell cavities (lumens), water vapor in the lumens, and liquid water bound in the cell wall. In

most practical uses, wood is in a dynamic state of absorbing and releasing the bound liquid-phase moisture in response to its changing environment. This range is the focus of the current research.

The other extreme moisture condition for wood is saturation. The point at which the cell walls of the wood are completely saturated without allowing water into the lumens is called the fiber saturation point (FSP). If the sample remains in a wet environment, it will continue to absorb moisture by filling the lumens. For this reason, the value of the moisture content of wood at the fiber saturation point is difficult to precisely determine.

The Sorption Isotherm

The graph of equilibrium moisture content at a given temperature over the entire relative humidity range is called the sorption isotherm. The dry state and a state near fiber saturation are generally the end points of the sorption isotherm. Brunauer (1943) defined five types of sorption isotherms and labelled them with Roman numerals. The type of isotherm that a particular material exhibits depends upon the dominant moisture transfer methods at different relative humidities. The five types are shown in Figs. 1 and 2.

Wood generally exhibits a Type II isotherm. This type of isotherm is also common among porous gels, including most food products. Three moisture transfer regimes can be seen in this type of isotherm, as shown in Fig. 3. As the relative humidity increases

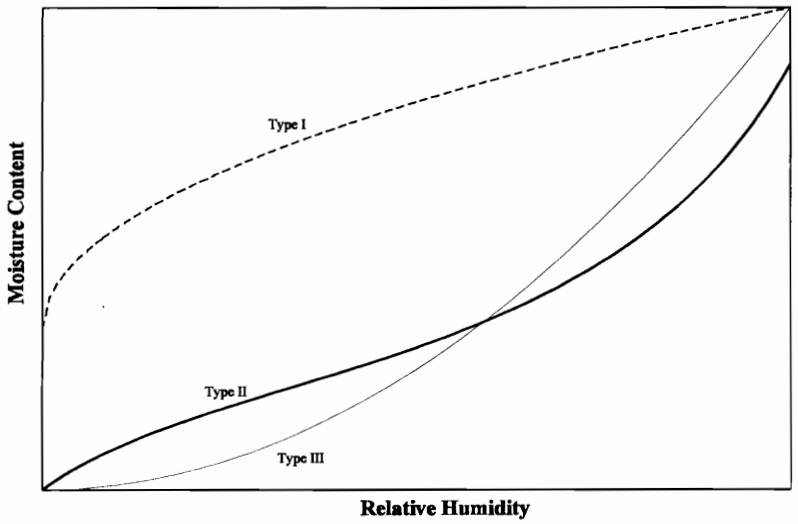

Figure 1. Type I, II, and III sorption isotherms.

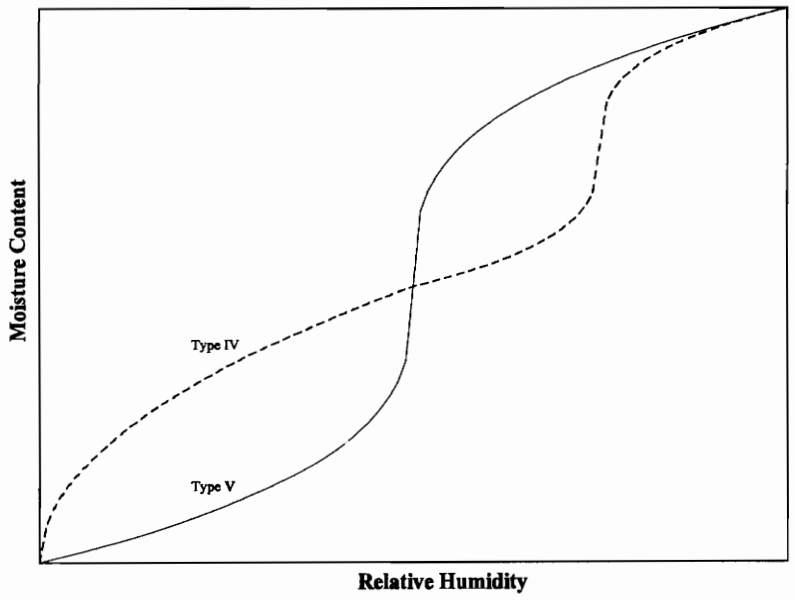

Figure 2. Type IV and V sorption isotherms.

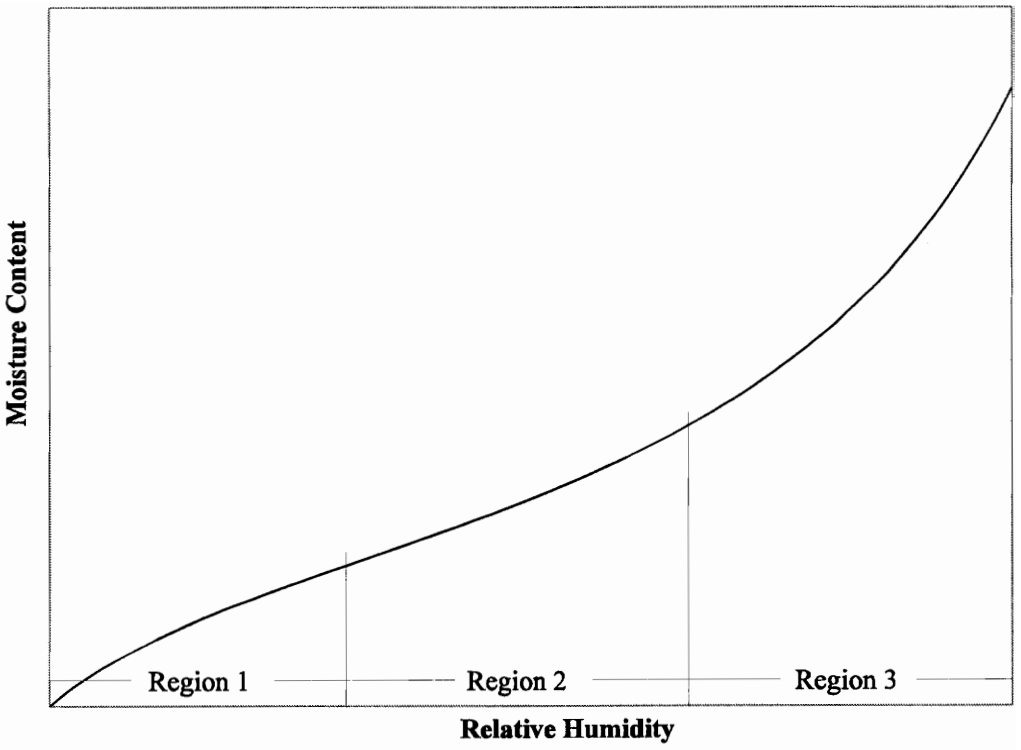

Figure 3. Type II sorption isotherm.

from zero in Region 1, the moisture content of the wood increases rapidly, but there is a "diminishing returns" effect. Region 3 shows the asymptotic approach to the fiber saturation point, and Region 2 is the nearly linear transition between Regions 1 and 3.

Creating a sorption isotherm involves plotting the equilibrium moisture content through a sequential set of relative humidities or vapor pressures. The fractional equilibrium moisture content is defined as:

$$\gamma = \frac{M_{eq} - M_{dry}}{M_{dry}}$$

Since the isotherm corresponds to equilibrium values, only steady-state information can be derived from it.

An example of the use of the sorption isotherm is the determination of differential heats of adsorption using the Clausius-Clapeyron equation (Brunauer, 1943). The general form of this equation is:

$$\left(\frac{dp}{dT}\right)_{sat} = \frac{s^{(2)} - s^{(1)}}{v^{(2)} - v^{(1)}}$$

where the superscripts denote the constant pressure and temperature phase change of water from vapor in the air to bound liquid in the cell wall of the wood. The change in entropy can be related to the enthalpy change by the "Tds" equation (Van Wylen and Sonntag,

1973):

$$dh = T\,ds + v\,dp$$

Condensation occurs at a constant temperature and pressure, so the dp term is zero, and the Clausius-Clapeyron equation assumes a solvable form:

$$\left(\frac{dp}{dT}\right)_{sat} = \frac{h^{(2)} - h^{(1)}}{T\,(v^{(2)} - v^{(1)})}$$

Further simplification of this equation is accomplished by replacing the specific volume of the vapor phase with v_g, which is much larger than that of the bound liquid phase. The specific volume of the liquid can be considered neglible compared with the specific volume of the vapor. Simplifying and rearranging the equation gives a simple form of the heat of adsorption per unit mass:

$$\Delta h_a = - Tv_g \left(\frac{dp}{dT}\right)_{sat}$$

The actual heat of adsorption can be determined by multiplying the right side of the equation by the mass of water vapor adsorbed, as follows:

$$\Delta H_a = - \gamma M_s T v_g \left(\frac{dp}{dT}\right)_{sat}$$

It should be noted that the saturation pressure in the above equation is not the vapor pressure of liquid water at the given temperature. Since the liquid is in the bound phase,

this pressure is the vapor pressure multiplied by the *activity* of the liquid. Thus, the heat of adsorption can be calculated if the moisture content of the sample is known. Given an accurate model of the sorption isotherm, it can be related to relative humidity of the sample's environment.

Hysteresis Effect. In the case of porous gels, such as wood, the sorption isotherm exhibits a hysteresis effect. The adsorption and desorption curves form the lower and upper limits, respectively, of equilibrium moisture content at given relative humidities and temperatures. The actual equilibrium moisture content is depends upon the immediate history of the sample's environment.

The ratio of the equilibrium moisture content values on the adsorption curve to the values on the desorption curve for various woods has been found to be in the 0.7 to 0.9 range for all measured data by Peters (1992), Okoh and Skaar (1980), and Peralta (1995a). Values between these curves are commonly found in practical applications of wood products, as a result of "scanning" caused by humidity fluctuation.

Scanning Curves. A complete scanning curve is a plot of equilibrium moisture content vs relative humidity which crosses the hysteresis band of the sorption isotherm. Scanning curves are useful for developing a model which will predict equilibrium moisture content based upon the recent history of the wood. Peralta (1995b) used his own scanning data

for yellow poplar (Peralta, 1995a), along with the independent-domain theory, to create such a model. Peralta's model requires that several scanning curves be determined for the precise case that is being modelled before it can be applied. In order for a model such as Peralta's to be useful, an enormous amount of data must be available.

Analytical and Empirical Models

There are several tools for researchers to use in deriving an moisture transfer in wood products. The first and most fundamental of these is applying the laws of conservation of mass and energy. This approach leads to coupled partial differential equations, which can be solved for a limited number of special cases, generally by using numerical methods. These coupled heat and mass transfer partial differential equations, as presented by Luikov and Mikhailov (1961), are shown below:

$$\rho c_q \frac{\delta T}{\delta t} = K_{qq}\nabla^2 T + K_{qm}\nabla^2 M$$

$$\rho c_m \frac{\delta M}{\delta t} = K_{mq}\nabla^2 T + K_{mm}\nabla^2 M$$

Gui, et al. (1994) used a finite element method to solve these equations for the case of wood drying. They were able to match existing experimental data for wood drying, but

they had to combine the heat and mass transfer coupling terms in order to solve the equations.

Another common approach is Fick's Law (Fick, 1855). The standard governing equation for mass transfer in porous media, which is known as Fick's First Law, is shown in one dimension below:

$$J_A = - D_A \frac{dC_A}{dx}$$

Fick's First Law is empirical and is limited to isobaric and isothermal single-phase diffusion. Variations of this law have been presented which reportedly eliminate these restrictions (Chevrier, 1996). In studying transient sorption in wood, Wadsö (1994) found Fick's Law to be applicable for small step changes in relative humidity up to 75 per cent, but not applicable for a relative humidity step change from 75 per cent to 84 per cent. He modelled the latter change as a phenomenon with a Fickian and a non-Fickian component. This model was further supported by Cunningham (1995), who labelled the non-Fickian element "anomalous" moisture sorption.

Darcy's Law has also been applied by some researchers. This law must be extended to encompass immiscible flow of two different fluids within in a solid medium. However, this approach has been shown to have problems of its own, especially in quantifying the viscous drag between the two fluids (Whitaker, 1986).

Another approach is to use a hybrid method between analytical laws and empirical

results. Berger and Pei (1973) formed a mathematical model of wood drying by using the Clausius-Clapeyron equation and a mathematical simulation of the sorption isotherm as coupling equations for the conservation laws. More recently, Peralta (1995b) presented a method for determining equilibrium moisture content in yellow poplar given the history of its environment which utilizes experimental results along with independent-domain theory.

Sorption data is used as input values for these moisture transfer models. These data may also be used to model the sorption isotherm as a function of material properties. Already, more than 200 equations that have been presented in an attempt to quantify the sorption isotherm (Leung, 1986).

General Moisture Transfer Theory. General conclusions about the nature of moisture sorption in wood have been reached through experimental as well as theoretical means. These two methods work together to allow a better understanding of the subject. The present data will provide more information for analytical researchers to use for quantifying some known phenomena.

The most fundamental problem in the numerical analysis of sorption is determining what moisture transfer methods can be neglected. Fortes and Okos (1980) list seven possible methods of moisture transfer. Of these, surface diffusion, diffusion driven by gravitational forces, and effusion are generally considered to be negligible. Liquid

diffusion, which is the flow of liquid forced by concentration gradients, was identified by Rosen (1987) as the principal mechanism involved when free water is removed from the sample. Babbitt (1950) theorized that the principal force in fluid diffusion in solids is total pressure differences. Capillary flow, which involves molecular attraction-driven liquid flow through interstices and on the surface of a solid, has been found to be significant at high relative humidities (Spolek and Plumb, 1980). A.V. Luikov is credited with discovering the seventh method of moisture transfer, which is vapor diffusion driven by temperature gradients. The temperature gradients cause partial vapor pressure gradients in the solid, which in turn drive fluid flow within the system. The coupling of moisture content and temperature gradients is known as the Soret effect (Ferguson and Lewis, 1993).

Analytical researchers can model sorption involving all of these moisture transport methods, but solutions to these models are extremely difficult and can only be achieved in highly simplified and specific cases. Experimental results are used to help identify the significant moisture transport methods. As more experimental data are obtained, the analytical models can possibly be simplified into a more manageable form. The object of all of this research is to create a few general methods which can be used to predict moisture content of porous gels for all cases.

Experimental Findings

An example of an experimental finding that gave a clue for analytical researchers was Wadsö's experiment (1994), which showed that Fickian diffusion did not hold well at high relative humidities. Cunningham (1995) quickly published an analytical model explaining the non-Fickian or "anomalous" moisture sorption. Another example was when Hedlin (1967) noted that sample weights became significantly more asymptotic above 60 per cent relative humidity. This observation showed researchers that some of the slower diffusion mechanisms control moisture transfer as the wood approaches the fiber saturation point.

Many models are first theorized by analytical researchers, then supported by experiment. An example of this interaction involves the coupling of heat and mass transfer. This problem was a major concern to analytical researchers since most coupled equations are extremely difficult to solve. Kumaran (1988) noted that this simultaneous heat and mass transfer modelling was especially difficult in cellulose materials as a result of the fact that condensed moisture transport can never be considered negligible in comparison with vapor transport. Kohonen (1984) agreed, citing the enormous amount of physical data necessary to accommodate the two inert components (solid, inert gas) and three water phases (vapor, surface adsorbent, capillary condensate) involved. However, he suggested that this work may not all be necessary, since his research showed that the

heat and moisture transfer coupling was not strong. This point was supported by the research of Gui, et al. (1994), in which numerical results agreed well with experimental data, despite the fact that the heat and mass transfer coupling terms were combined into a single term.

Scope of the Research

The current research involves the improvement of an existing experimental method, which was shown to be an effective method by Peters (1992). The performance parameters that can be improved are the relative humidity and temperature ranges and the control mechanism. The current maximum and minimum relative humidity boundaries for Peters' apparatus at near-ambient conditions (20.8 C) were 85 per cent and 0.4 per cent, respectively. He did not explore temperature range and humidity limits at various temperatures.

The primary goal of the current research is to investigate and increase the range of operation of the existing apparatus. The control and precision of the measurements is another goal of the research. Specific goals are to get sorption isotherm data for exterior grade plywood, oriented strand board, and fiber board sheathing at 5 C, 25 C, and 55 C and scanning curve data from the 50 per cent relative humidity set point on the adsorption and desorption curves for the 25 C isotherms.

EXPERIMENTAL APPARATUS AND PROCEDURE

The experimental apparatus is composed of a test chamber with an external forced-air temperature and humidity control system. Instrumentation to monitor dry bulb temperature, relative humidity, and dew point are included in the system. Material samples are placed in open aluminum dishes within the test chamber, and the mass is determined in situ by suspending the aluminum dishes from an electronic balance located directly above the test chamber. The apparatus is shown schematically in Fig. 4 and photographically in Fig. 5.

Test Chamber

The material of the test chamber is acrylic, which was chosen because of its translucency, nonhygroscopicity, and low thermal conductivity. The fact that it is nonhygroscopic and has a low thermal conductivity is important in achieving effective relative humidity and temperature control with a minimum of input energy. One inch thick black polymer foam insulation surrounds the chamber, further reducing the heat

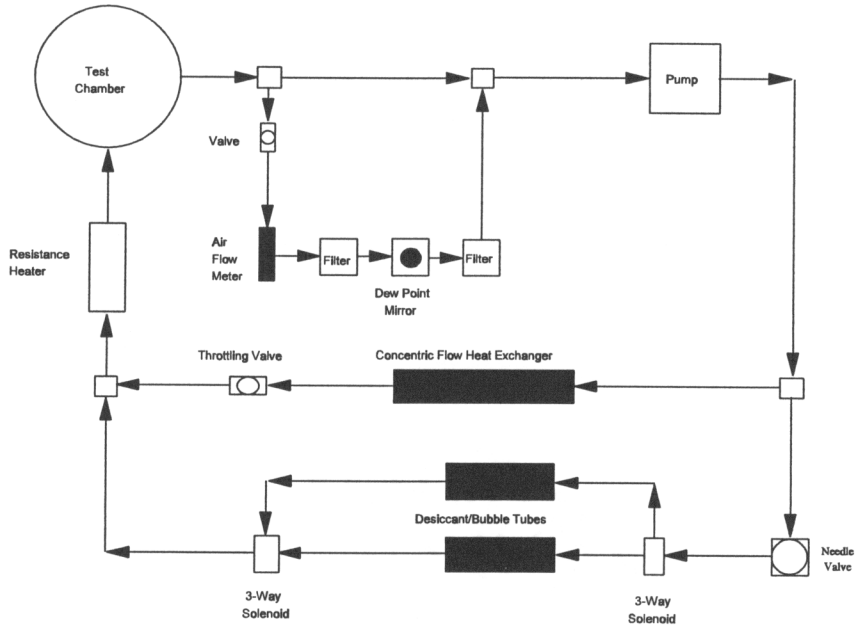

Figure 4. Schematic diagram of the experimental apparatus.

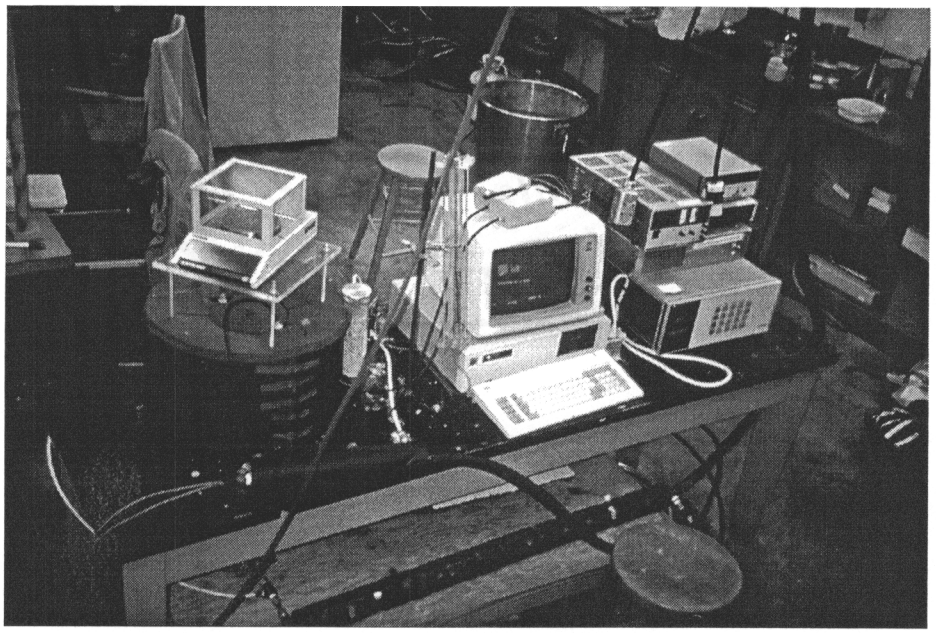

Figure 5. Photograph of the experimental apparatus.

transfer between the inside of the chamber and the ambient air. The nominal thermal conductivity of the insulation is 0.036 W/m-K.

The test chamber is 12 inches outside diameter with a 1/4 inch nominal wall thickness. This size creates an interior which is capable of handling 6 aluminum "boats" of 3-inch diameter simultaneously. The test chamber is 9-1/2 inches high, which gives sufficient room for moving the test specimens for mass measurement. The dimensions of the test chamber were chosen in order to allow for easy access to the test specimens while minimizing the volume which requires temperature and relative humidity control.

The bottom part of the chamber is attached to an acrylic flange with solvent cement. This flange is bolted to the top plate of the chamber with a 1/8 inch thick nitrile rubber gasket separating them. On the top of the chamber and below the flange are aluminum rings, which serve to distribute the pressure of the 12 bolts evenly around the diameter.

The top of the chamber is designed to allow access to the test specimens. Specimens are placed in and removed from the chamber by removing the bolts and lifting the top. Mass measurement in situ is allowed through use of the 1/4 inch pipe (ips) hole tapped in the center of the plate. This hole is plugged during normal operation.

Two other 1/4 ips holes are tapped into the top plate, which are used to insert relative humidity sensors (Vaisala RH&T HMP Probes 12 and 13) into the chamber. The sensors are sealed into the chamber with wax. A thermocouple is inserted into the

chamber for measuring dry bulb temperature. These are all attached to the side of the bottom part of the chamber.

External Conditioning System

Inlet and outlet connections to the test chamber allow air flow through the external conditioning system. Air is circulated from the chamber through temperature and humidity control sections and back to the chamber in order to maintain specified environmental conditions within the chamber. The direction of flow in the external conditioning system is shown in the schematic diagram of the apparatus, Fig. 4. The pump circulates the air through the system. Air leaves the chamber and goes into the pump. On the way to the pump, a small amount is directed through the dew point hygrometer. The air that goes through the hygrometer is regulated by a needle valve and cleaned by filters before and after the dew point reading. It then rejoins the flow into the pump. Upon leaving the pump, the air flows toward the concentric tube heat exchanger. Once again, a small amount is diverted, this time being sent through the humidity control section. In the humidity control section, moisture is added or removed in order to maintain the desired humidity in the test chamber. The rest of the air flows through the concentric tube heat exchanger, where it is heated or cooled to just below the desired temperature, and through the back pressure valve, which exerts enough pressure to insure

that there is sufficient flow through the humidity control section. The main air flow then enters the resistance heater, where it is rejoined by air leaving the humidity control section. At the exit of the resistance heater, the air re-enters the chamber at the proper humidity and temperature to effect control.

Circulation. Circulation is forced by a Parker Metal Bellows MB-602 pump, which was chosen because it minimizes leakage of system air. The forced air movement allows active control of environmental conditions in the chamber and increases the rate at which test specimens achieve equilibrium moisture content at each set point. The tubing through which the system air flows is constructed of a thermoplastic material known as Impolene™. This material is highly nonhygroscopic and somewhat flexible, which makes it easy to use.

Test Chamber Temperature Control

The temperature in the test chamber is controlled by forcing air through a concentric flow heat exchanger and a resistance heater in series. Air leaving the test chamber is heated by the inefficiencies in the pump, and then must be cooled by the concentric-tube heat exchanger to slightly below the set point. At the surface of this heat exchanger, the air is at the lowest temperature that it will reach within the system, so the

temperature of the coolant water determines the maximum relative humidity achievable before condensation occurs. For this reason, the heat exchanger used is a copper tube with integral machined fins to enhance heat transfer. Since the heat transfer between the heat exchanger and the air is maximized, the coolant temperature can be set closer to the set point of the test chamber, which allows a higher maximum relative humidity in the chamber without condensation forming.

The coolant referred to in the preceding paragraph is actually a 40 per cent ethylene glycol-water solution. This solution is supplied to the concentric flow heat exchanger by a Forma Scientific Model 2425 Bath and Circulator. The bath has a range from -29 C to +70 C, and can be set in increments of 0.1 C. The manufacturer stated control sensitivity is $\pm$ 0.02 C. The bath, which pumps the ethylene glycol solution to the apparatus from outside of the laboratory, is shown in Fig. 6.

From the concentric flow heat exchanger, the air enters the resistance heater to be heated up to the temperature set point of the test chamber. The resistance heater can supply 120 W, but its use must be minimized, as described above. The resistance heater is controlled by the GW-BASIC control program used to automatically operate the system. The temperature is read by the program and compared to the set point. Using this comparison, the program sends information through the Hewlett Packard Isolated DAC/Power Supply Programmer for the Kepco JQE Power Supply to increase or decrease the voltage sent to the resistance heater. The control program controls the temperature to

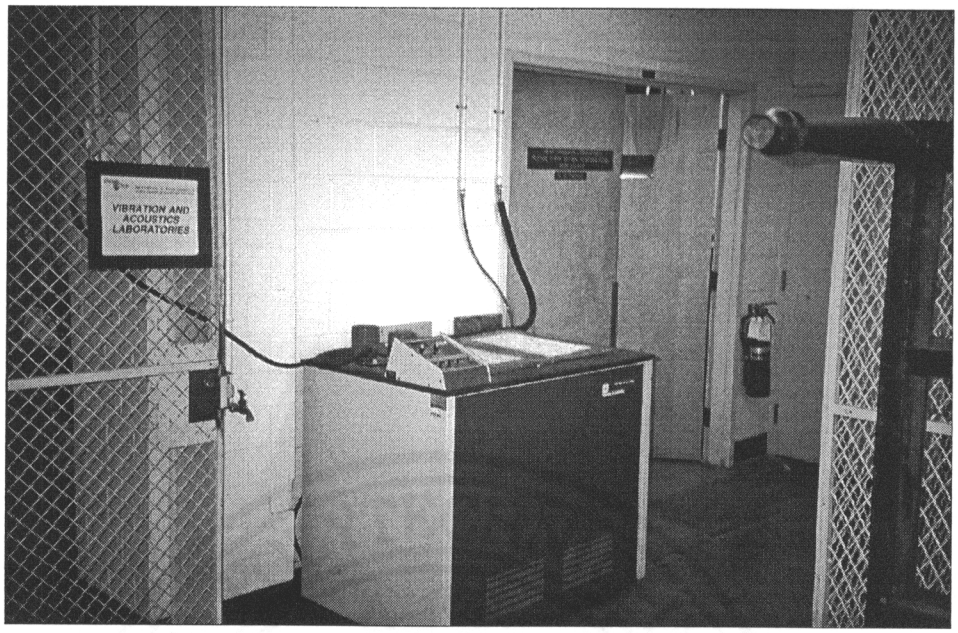

Figure 6. Photograph of the temperature bath and circulator.

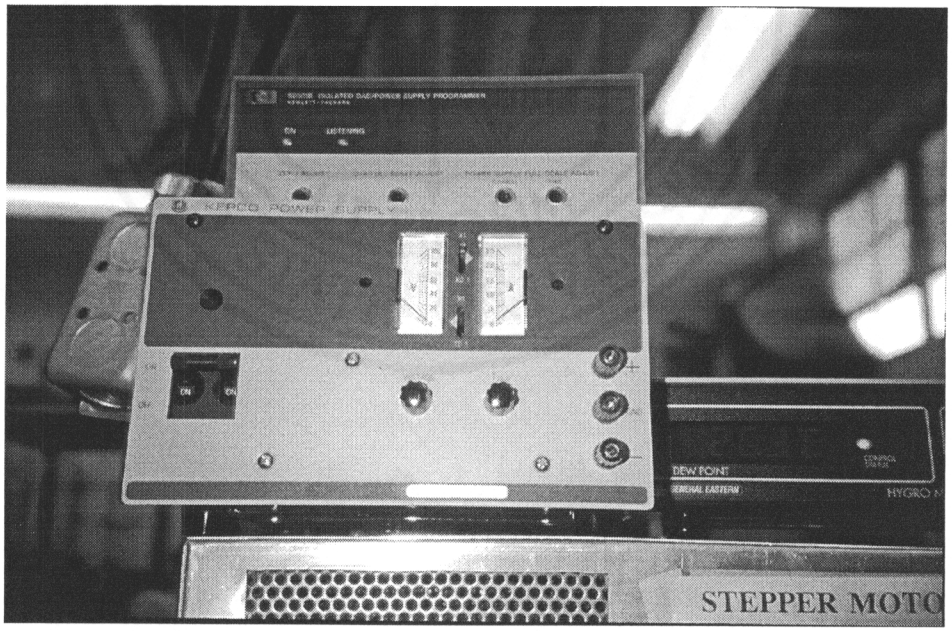

Figure 7. Photograph of the power supply and power supply programmer.

within $\pm$ 0.1 C. The power supply and power supply programmer are shown in Fig. 7.

Temperature measurement. Dry bulb temperature in the test chamber is determined using a type T (copper-constantan) 24 AWG standard thermocouple. The voltage across the thermocouple is measured with a Hewlett Packard 3497A Data Acquisition/Control Unit. The data acquisition unit is capable of reading DC voltages from 1μV to 120V, and has a control sensitivity of 1μV. The GW-BASIC control program converts this voltage into a Celsius temperature using Newton-Raphson iteration. Included in the data reduction procedure is an equation from NBS Monograph 125 (Powell, et al., 1974). The thermocouple was calibrated using NIST traceable thermometers, and the resulting calibration curve was included in the control program.

Test Chamber Relative Humidity Control

Relative humidity control in the test chamber is effected by sending some of the system air through either a "bubble tube" (Stamm, 1964) or a desiccant tube. Unlike the temperature control section, the relative humidity control section can achieve control with only a small percentage of the total system air. This air is diverted just before the concentric tube heat exchanger, and it rejoins the system air just before the resistance heater. It is important that this air does not pass through the concentric tube heat

exchanger, because of the risk of condensation in the bubble tube. If the air went through the concentric tube heat exchanger, it would be slightly below the test chamber set point, and there would be a risk of condensation at higher relative humidities.

A Superior Electric Slo-Syn^{R} Synchronous/Stepping Motor is used to rotate a metering valve to regulate flow through the bubble or desiccant tube. The stepper motor is controlled by increments of 1 step, where 200 steps is one revolution, and approximately 20 revolutions will bring the valve from fully closed to fully open. Control of the stepper motor is achieved through the GW-BASIC control program. The control program sends information to a Computer Continuum LAB 40-PC Host Adaptor Interface Card, which controls the Computer Continuum LAB 40-5 Four Axis Stepper Driver. The stepper driver turns the stepper motor valve, allowing more or less air to flow through the relative humidity control section.

As air enters the humidity control section, it first goes through the stepper motor valve. From there, the air enters the first of two three-way solenoids, which are regulated by the GW-BASIC control program as designed by Coudon (1994). The control program turns the solenoids on and off through the use of the Hewlett Packard 3497A Data Acquisition/Control Unit. Whether the solenoids are on or off determines whether the air will enter the bubble or desiccant tube. After passing through its designated tube, the air enters the other three-way solenoid and exits the relative humidity control section.

Bubble and Desiccant Tubes. The bubble tube is an acrylic tube containing distilled water that is used to add water vapor to the system air. This addition is accomplished by the configuration of the inlet and outlet of the tube. Air enters the tube from the top. A thin copper pipe forces the air to the bottom of the tube, under the surface of the water. At the bottom of the tube, the air is released, which allows it to bubble to the surface of the water and enter a second thin copper pipe at the top of the tube. This pipe guides the humidified air out of the bubble tube through the bottom. This design allows water vapor to enter the system while preventing liquid water from getting in the system when it is shut down.

The desiccant tube is also made of acrylic, and its function is removing moisture from the system. The tube is manufactured by W. H. Hammond Drierite Co., for the Drierite Model L68GP Gas Purifier. The desiccant in use, however, is a Davison Chemical 4 Å effective pore size molecular sieve. This effective pore size allows the desiccant to adsorb objects on the order of the size of water molecules (critical diameter 2.6 Å). The molecular sieves have a crystalline structure incorporating alumina tetrahedra and silica, and are useful in low pressure air drying, due to the fact that the heat release involved does not affect their performance.

Relative humidity measurement. Two separate methods are used to determine relative humidity in the chamber. A Vaisala RH&T Probe HMP 123B and a Vaisala RH&T Probe

HMP 133Y are used to directly measure relative humidity in the chamber. The stated accuracy of these probes is $\pm$ 2 per cent at relative humidities less than 90 per cent, and $\pm$ 3 per cent above 90 per cent relative humidity. They can be used in environments from -20 C to +80 C. Additional error for temperature change is $\pm$ 0.3 per cent RH/K. The Vaisala relative humidity probe was chosen primarily for its short response time and excellent reliability which allows more precise control over long terms compared with the dew point hygrometer. The probes are inserted into the top of the chamber, as shown in Fig. 8.

The more accurate method of relative humidity measurement used was the General Eastern Model D-2X Dew Point Hygrometer. The hygrometer contains a chiller mirror

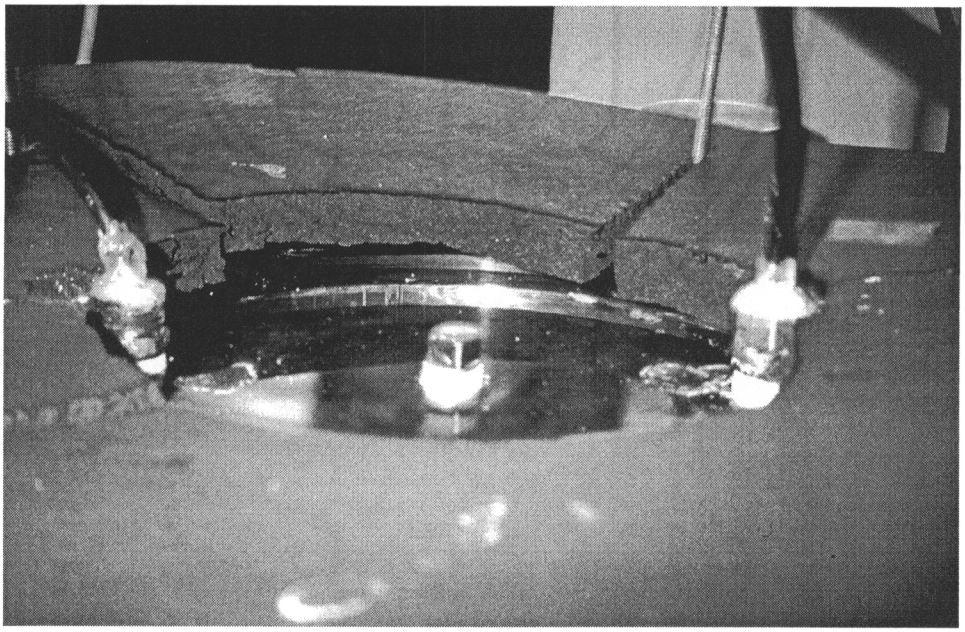

Figure 8. View of Vaisala probes inserted in chamber.

that cools a small portion of the system air that passes through it until condensation forms. This temperature is converted to a voltage to the General Eastern Hygro M1 Dew Point Monitor and the Hewlett Packard Model 3497A Data Acquisition/Control Unit. The control program converts the voltage into a dew-point temperature, and uses this and the test chamber dry-bulb temperature to calculate relative humidity. Vapor pressures, which are determined using correlations by Goff and Gratch (1946), are used in the relation

$$RH = \frac{P_v(T_{dp})}{P_v(T_{db})} \; x \; 100$$

to calculate the relative humidity in the chamber. The dew point measurement system is shown in Figs. 9 and 10.

The stated accuracy of the dew point hygrometer is $\pm$ 0.1 C, and it is usable over a range from -25 C to +80 C. It is used to calibrate and check the accuracy of the Vaisala relative humidity measurements. However, the dew point measurement is much slower than the Vaisala to react to changes in test chamber humidity, so it is not as good for precise control. The dew-point chilled mirror is also not designed for continuous use, and it is very sensitive to contaminants or water in the system. It is for these reasons that the Vaisala relative humidity probes are used for primary control of the test chamber relative humidity.

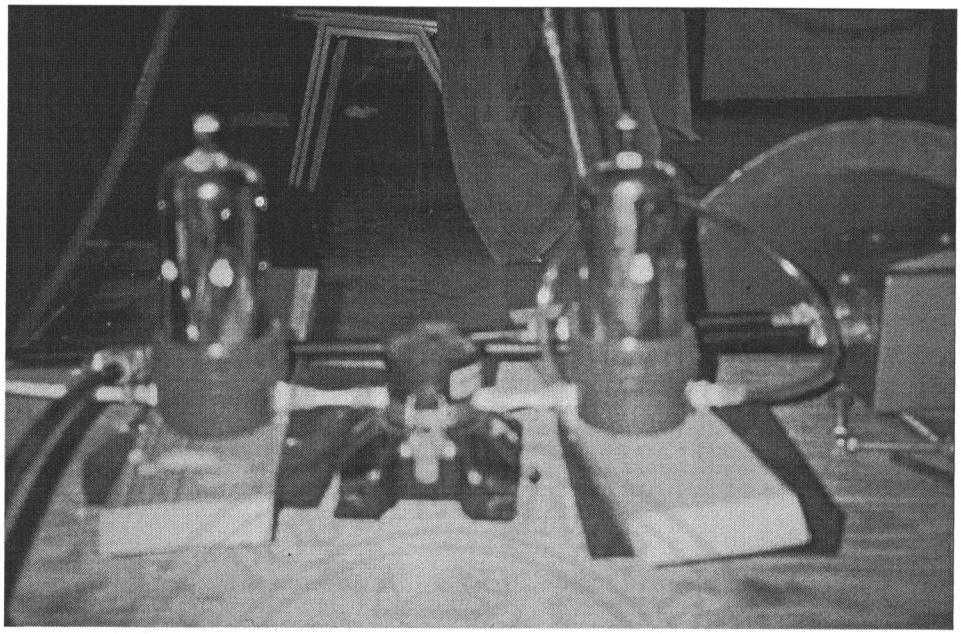

Figure 9. Photograph of the dew point hygrometer with two filters.

Figure 10. Photograph of the dew point monitor.

Automated Control of Temperature and Relative Humidity

The control program controls the temperature and relative humidity of the test chamber in a single loop. Upon executing the control program, the user is asked to input initial parameters, which are the relative humidity and temperature set points and initial positions for the stepper motor and power supply programmer. These allow the program to be stopped and restarted without losing continuity of control. Proportional, integral, and derivative control coefficients are calculated for the stepper motor movement and the power supply voltage output.

Control Algorithm. A single control algorithm was used for the control of both the relative humidity and the temperature in the test chamber. The algorithm chosen contains proportional and derivative control, with a modified form of integral control. Standard integral control could not be used, because of the onset of "integral windup" error caused by changes in set point. Integral windup occurs when the control program builds up a large integral below or above the set point. When this situation occurs, the integral causes a large overshoot, and a very slow damping of the measured value to the set point. Because of this limitation, integral control is not enabled until the measured relative humidity is within $\pm$ 0.5 per cent or the measured temperature is within $\pm$ 0.4 C, and it is reset to zero when the measured value crosses the set point. The primary purpose of

the integral control is to avoid an offset which is too small for the proportional control to eliminate.

Proportional control is the driving force of the control program. This type of control forces the measured value toward the set point, until it is close enough for integral and derivative control to take over. Derivative control is used to flatten the measured value curve and avoid overshoot. If the slope of the measured values is too great in relation to its distance from the set point, then the derivative control acts against the proportional control and causes the measured value to approach the set point more slowly. The control equation is for a proportional-integral-derivative (PID) controller as described by Smith and Corripio (1985):

$$m(t) = m_0 + K_c e(t) + \frac{K_c}{\tau_I}\int e(t)dt + K_c \tau_D \frac{de(t)}{dt}$$

where m is the controlled variable and m_0 denotes the previous value of the controlled variable. The result is rounded to the nearest integer and implemented physically. The power supply programmer value increases or decreases the voltage supplied to the resistance heater by the power supply, while the stepper motor value gives the number of steps the valve will turn. The control algorithm also decides whether the three-way solenoids will be on or off, and sets maximum and minimum values for the stepper motor and power supply programmer. The details of the control program can be found in

Appendix B. Control coefficients were determined by trial and error.

Equilibrium Moisture Content

The direct gravimetric method is used in the determination of moisture content. Wood specimens are weighed in situ at intervals of 6-12 hours until no change in mass can be detected. At this point, the specimens are considered to have reached equilibrium. The equilibrium moisture content is expressed in terms of the dry mass, which is determined during the test run at the minimum relative humidity attainable by the apparatus. The minimum relative humidity is typically less than 0.2 per cent.

Mass measurement. The mass of each test specimen is determined in situ, which allows environmental changes in the chamber to be minimized. Every 6-12 hours, the mass of each of the six specimens in the chamber is recorded. In order to accomplish this measurement, the pump is first turned off. (If the pump were left on, the mixing of the system air and ambient air would be forced, which would cause the system air to approach ambient conditions more quickly. Leaving the pump on would also cause fluctuation of the mass measurement.) The next step is to turn off the Kepco power supply. This step is important because the air in the system is now still, and the resistance heater will heat it to well above the temperature set point before the pump is restarted. After these are

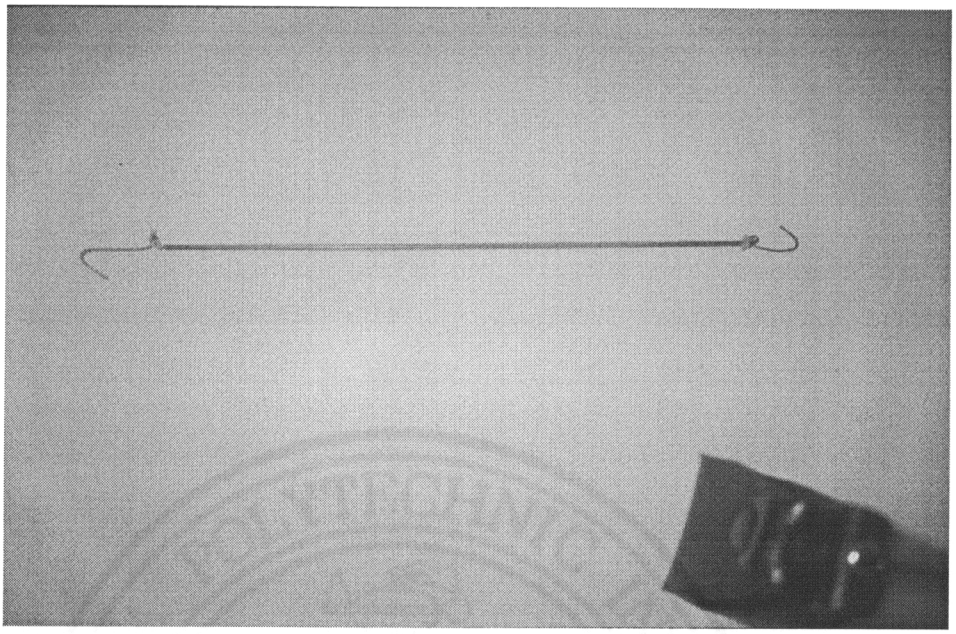

Figure 11. Photograph of hook used to maneuver and weigh specimens.

turned off, the test chamber can be opened by unscrewing a 1/4 ips plug in the top with minimal mixing of ambient and system air. A thin wire hook, shown in Fig. 11, is then used to hook the handle of each aluminum weigh boat and suspend them one at a time from an electronic balance. The electronic balance is placed above the chamber on a platform. This configuration is shown in Fig. 12.

The electronic balance used is a Mettler PM400 precision balance. This balance can measure masses between 0 and 410 g in increments of 0.001 g, and has a reproducibility of 0.001 g. The linearity of the scale is $\pm$ 0.002. The minimum specimen dry mass is 3.0 g, which corresponds to an uncertainty of less than 0.001 kg water/kg dry mass in moisture content. Therefore, the maximum uncertainty of the dry mass as defined

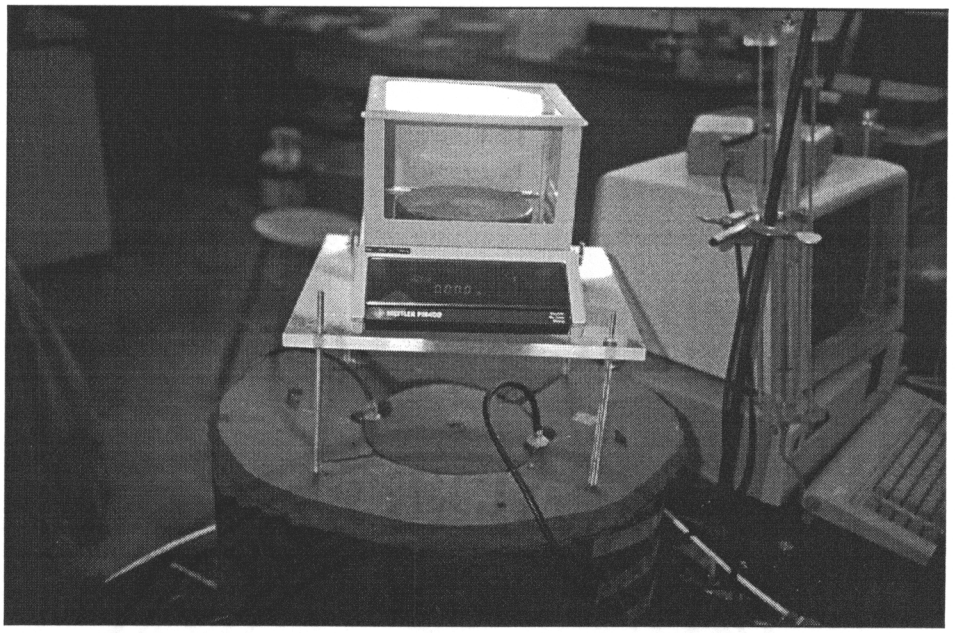

Figure 12. Photograph of the electronic scale mounted above test chamber.

in the context of the present experiment is 3 per cent.

Masses of the test specimens are measured every 6-12 hours until no change in mass can be detected. Measurements taken 48 hours after this point during a test run proved that the moisture content does not change significantly after this point. Moisture content changes on the order of 0.001 g occur in a six hour interval after approximately 12 hours at low relative humidity and 18 hours at higher humidities during room temperature adsorption.

Specimen containers. The test specimens are placed in aluminum weighing dishes, which have a diameter of 2-3/4 in and a depth of 3/4 in. These dishes are light weight,

nonhygroscopic, and capable of holding up to 6 grams of dry specimen, which easily allows an accurate measurement without risk of particles falling out of the dish. Aluminum wire is attached across the diameter of each dish, which allows the specimens to be retrieved with the thin wire hook described previously. The containers each have a mass on the order of 2 grams, and are marked for identification. Six containers can be fit into the chamber at one time, as shown in Fig. 13.

Determination of dry mass. The dry mass of each specimen is determined by diverting nearly all of the system air through the desiccant tube. A small amount of air is allowed to run through the concentric flow heat exchanger in order to maintain temperature

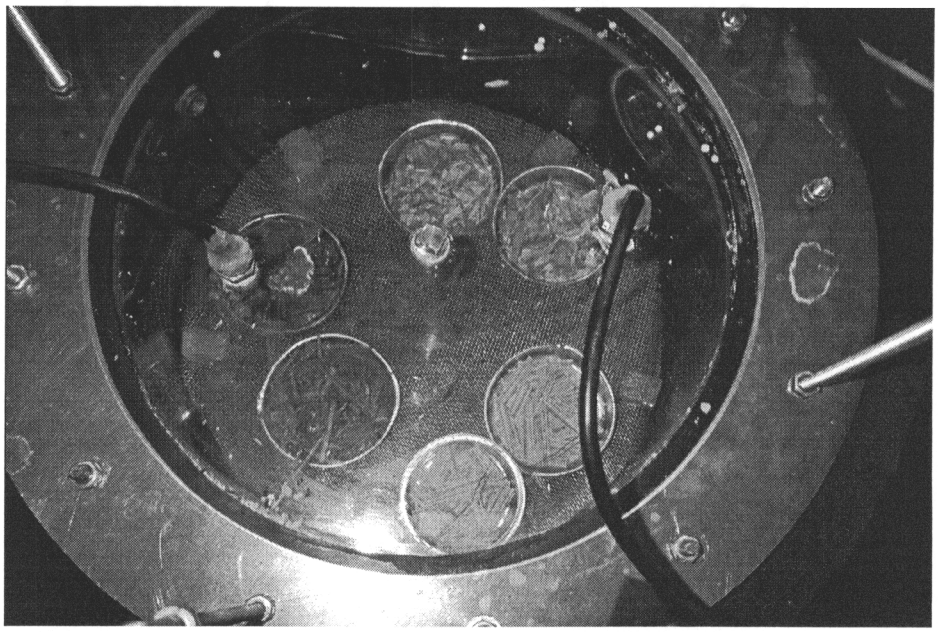

Figure 13. Photograph of the test chamber with six samples inside.

control. This task is accomplished by closing the back pressure valve and opening the stepper motor as much as possible. This method creates a minimum relative humidity in the chamber, which is less than 0.1 per cent, according to the Vaisala probes. The dew point hygrometer cannot measure values as low as those created in the chamber at this humidity. The accurate value of the relative humidity in the chamber cannot be determined, due to the uncertainty of the measurements, but is generally assumed to be less than 0.5 per cent. The dry mass is determined by using the mass measurement technique described above at this relative humidity.

This method is desirable because it does not involve heating of the wood specimens. Stamm (1964) found that exposing wood to elevated temperatures may cause it to lose some of its cell-locked water, which cannot be replaced. Oven drying can lead to significant error, according to the findings of Richards, et al. (1992). Peters (1992) used these findings to show that an oven-dried sample of southern pine with a dry mass of 5.5 g would have a 13.3 per cent error in moisture content at 75 per cent relative humidity.

Experimental Procedure

The test procedure was developed by Peters (1992), with uniformity of test chamber conditions being the primary focus. This objective was achieved by determining

all moisture contents in situ, and allowing minimal contact between the test specimens and the ambient air. In order to achieve these conditions, all of the moisture content data had to be found in a minimum number of test runs. The solution was to initially saturate the specimens with water and proceed from maximum relative humidity in the test chamber down to minimum relative humidity in steps, and similarly back up to maximum relative humidity. This procedure allows the measurement of the entire adsorption and desorption curves in a single test run. The desorption curve and the adsorption curve meet at 0 per cent relative humidity and above the fiber saturation point, and form the boundaries of moisture content below the fiber saturation point of each specimen.

Test specimen preparation. Maximizing the surface area of the specimens minimizes the time required to reach equilibrium moisture content. Richards, et al. (1992) concluded that reducing the specimen size reduces the time to reach equilibrium while having a negligible effect upon the value of the equilibrium moisture content. Christensen (1960) found that using samples as thin as 180 μm (0.007 in) had little effect upon the moisture content results. The important factors in determining the test specimen size were whether the specimen was representative of the whole (Simpson et al., 1994) and whether each piece could withstand the flow in the chamber without being blown out of its aluminum weigh boat. Thin slices of each of the materials were cut with a table saw to approximately 0.03 in thick, which was the minimum effective thickness attainable. An

attempt was made to use a microtome, which could cut slices with a maximum thickness of 100 microns (0.004 in), but the specimens fell apart. The specimens used in this experiment were all composite woods, so care was taken to preserve the connective material as well as the wood.

Saturation of specimens. Before the specimens are placed in the chamber, they are saturated with water. The specimens are first placed in a desiccator jar with distilled water, and a vacuum pump removes all of the trapped air from the specimens and the water. The specimens are then removed and placed in airtight jars and submerged in the water from the desiccator jar. After being submerged for 12 hours, the specimens are defined as saturated in the context of this experiment.

There is not a definite point of saturation, since the water will continue to absorb moisture in the cell cavities long after reaching the fiber saturation point. A moisture content above the moisture content at the maximum relative humidity of the chamber is sufficient for use as saturated in this experiment. The fiber saturation point is known for most woods to be around 30 per cent moisture content. The samples are saturated to start the test run because the test chamber is capable of approaching 0 per cent relative humidity much closer than it is of approaching 100 per cent relative humidity, because of the onset of condensation in the system at high humidities.

Sorption isotherm. The sorption isotherm is the plot of the curve of moisture content vs relative humidity which contains the adsorption and desorption curves at a given temperature. The relative humidity is the independent variable, and is decreased from the maximum attainable by the test chamber to the minimum attainable by the test chamber in steps, and is then increased in steps back to the maximum attainable by the test chamber. The equilibrium moisture content is determined at each set point. These set points were chosen symmetrically about 50 per cent, and are as follows: 10, 20, 30, 40, 50, 60, 70, 80, and 90 per cent relative humidity. The minimum relative humidity attainable by the chamber is considered 0 per cent and the initial saturated state described above is considered 100 per cent. This process has been repeated for sorption isotherms of the three test materials at 12 C, 25 C, and 55 C.

Scanning curves. Scanning curves are curves from one boundary of the sorption isotherm to the other. These are typical of wood in a natural seasonal environment. Scanning curves were determined at 25 C for the specimens from 50 per cent relative humidity on the adsorption curve to the desorption curve, and from 50 per cent relative humidity on the desorption curve to the adsorption curve. These curves are determined by first plotting the sorption isotherm, then drying or saturating the specimen as needed. The test chamber is then set to the relative humidity desired for the start of the scanning curve. The specimens should reach an equilibrium moisture content consistent with the starting

boundary curve on the sorption isotherm. The test chamber relative humidity is then increased or decreased in the same steps as the sorption isotherm until the moisture content reaches the other boundary curve.

RESULTS AND DISCUSSION

The sorption isotherms of exterior grade siding (EGS), oriented strand board (OSB), and fiber board sheathing (FBS) have been measured for temperatures of 12 C, 25 C, and 55 C. Each of these isotherms was compared with typical moisture content data from the Forest Products Laboratory. Scanning curves for the 25 C sorption isotherms were produced from the 50 per cent relative humidity set point on both the adsorption and desorption curves. Suggestions are made to extend the operating range of the apparatus.

Performance Capabilities of the Apparatus

The temperature of the test chamber can be maintained at temperatures between 10 C and 70 C. The limitation for the minimum temperature is the insulation of the system. Some parts of the system are difficult to effectively insulate, including the flow control valves, the bubble tube, and the desiccant tube. The distilled water and the desiccant in the relative humidity control section remain at room temperature, which affects the temperature of the air passing through this section. The low temperature experiment was

performed at 12 C to allow control by the resistance heater. The maximum chamber temperature is limited by the maximum service temperature of the tubing, fittings, and instruments.

The maximum relative humidity was the limiting factor for the operating range at each temperature set point. For all of the temperatures, the minimum relative humidity was indistinguishable from zero percent with the equipment used. At 25 C, the maximum relative humidity attainable was in excess of 90 per cent, which is a significant improvement from Peters' maximum of 85 per cent at 20.8 C. The 12 C run reached a maximum of 80 per cent relative humidity. A major performance limitation appeared at 55 C, when condensation formed in the test chamber at 40 per cent relative humidity. This problem is a consequence of experimental procedure. When the conditioning system is shut off and the test chamber is opened for weighing the samples, the ambient air cools the inside surface of the test chamber below the dew point of the air inside, causing condensation to form.

In an attempt to increase the operating range of the apparatus, the dew point hygrometer loop was removed from the system to reduce heat losses. The entrance to the relative humidity control section was moved downstream of the concentric tube counterflow heat exchanger, so the air flowing through this section would be as close to the test chamber temperature set point as possible. This configuration of the system is shown schematically in Fig. 14.

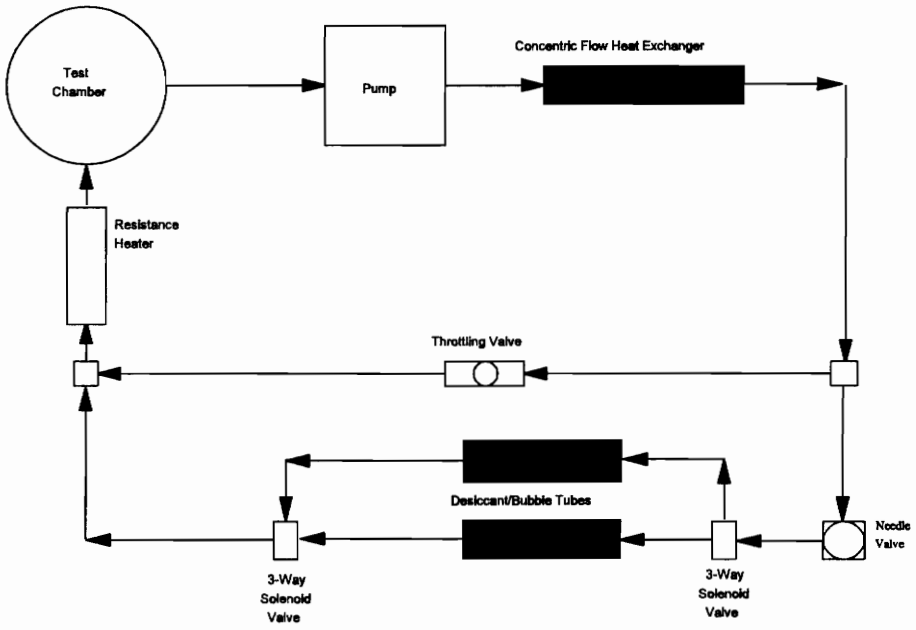

Figure 14. Schematic diagram of the apparatus configured for extreme temperatures.

Long-term control of test chamber relative humidity and temperature. The time-averaged control of the apparatus was significantly improved. A preliminary experiment was run to reproduce the set points from the previous experiment by Peters. Samples were weighed every 6-12 hours to assure consistency with a real experiment. Results of the improved apparatus are shown in Table 1, and Table 2 shows Peters (1992) results. For the new apparatus, the overall mean temperature was 25.000 C and the standard deviation was 0.0018 C, compared to the maximum standard deviation of 0.14 C in Peters' experiment.

Equilibrium moisture contents at lower relative humidities were typically achieved in 24 hours for adsorption and 36 hours for desorption for the 25 C run. As the relative

Table 1. Test chamber control and precision data for the current apparatus.

RH Set Pt (%)	RH Mean (%)	RH Standard Dev	T Mean (C)
0	0.0717	0.0166	25.007
15	15.033	0.0409	24.991
25	25.005	0.0472	24.996
35	35.003	0.0551	25.002
50	50.002	0.0456	25.002
65	65.002	0.0422	25.002
75	75.000	0.1208	24.998
85	85.024	0.1627	25.001

Table 2. Previous test chamber control and precision data (Peters, 1992).

RH Set Pt (%)	RH Mean (%)	RH St Dev	T Mean (C)	T St Dev
0.4	0.375	0.040	20.865	0.125
15	14.971	0.226	20.771	0.055
25	24.989	0.152	20.823	0.124
35	34.995	0.166	20.836	0.108
50	49.995	0.147	20.860	0.100
65	64.993	0.139	20.801	0.085
75	74.995	0.169	20.831	0.066
84	84.075	0.683	20.812	0.063

humidity increases, the time to reach equilibrium increases. At high relative humidities, equilibrium moisture content is reached in about twice the time as compared to lower relative humidities. Temperature also has a significant effect upon the time to reach equilibrium. The points attained in the 55 C run showed settling times of 12-18 hours on the adsorption curve and 18-24 hours on the desorption curve. At 12 C, these times were 30-60 hours for adsorption and 36-72 hours for desorption.

Short-term control of test chamber relative humidity and temperature. Control of relative humidity and temperature of the test chamber at each point is vital to obtaining reliable sorption data (Stamm, 1964). The current apparatus maintains environmental conditions to well within the uncertainties of the measuring instruments. Graphs of the control of the system at 50 per cent relative humidity and 25 C are shown in Figs. 15 and 16 . The test chamber humidity and dry bulb temperature were recorded once per minute.

The other factor affecting the short-term control of the environmental conditions in the test chamber is the system's response to a step change in the humidity set point. The current control program is designed to reach a new set point quickly and with no overshoot. The elimination of fluctuation and overshoot ensures that there is no deviation from the isotherm, whether adsorption or desorption. A graph of typical system response to a step change in the relative humidity set point from 50 per cent to 65 per cent is shown in Fig. 17.

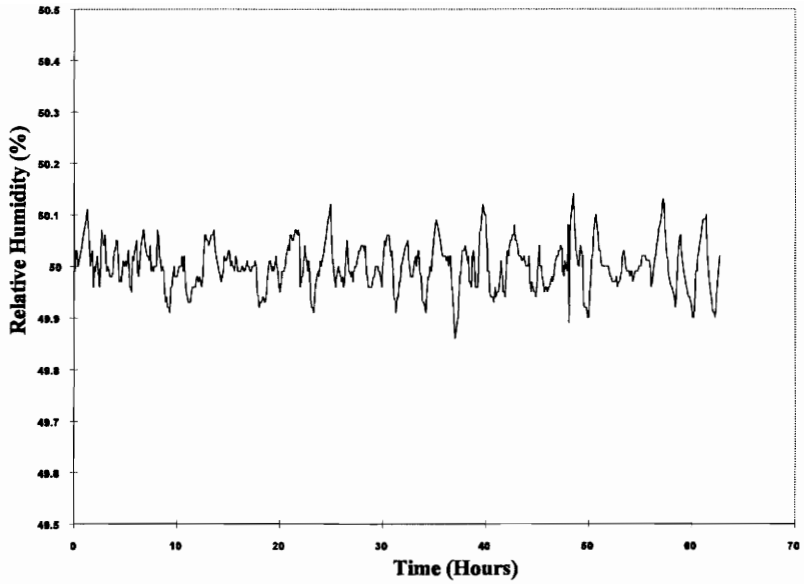

Figure 15. Stability of test chamber relative humidity.

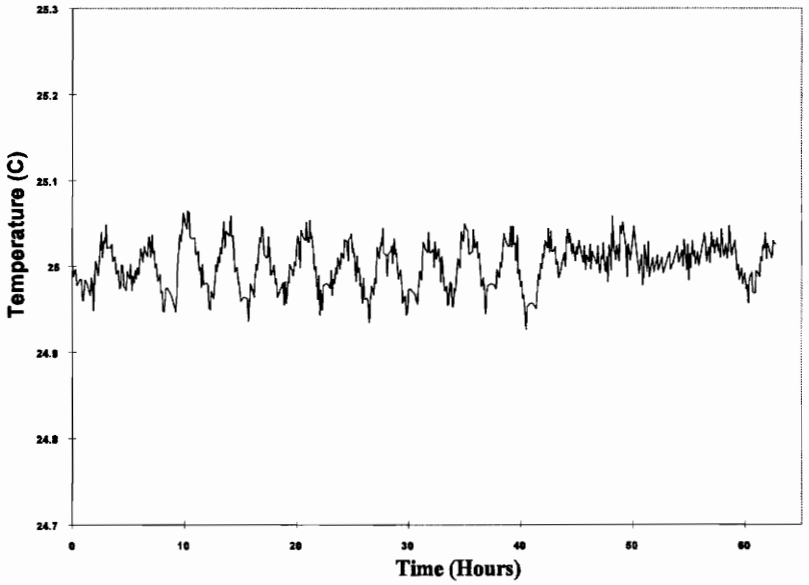

Figure 16. Stability of test chamber temperature.

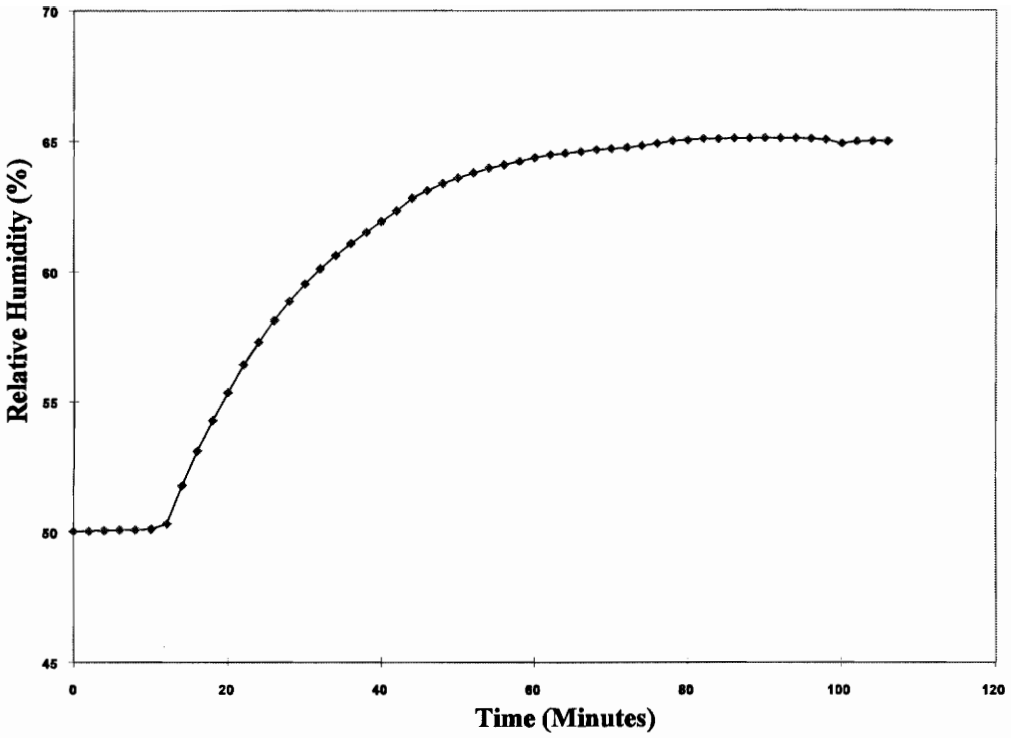

Figure 17. System response to a step change in relative humidity from 50 to 65%.

Maximum test chamber relative humidity. The limiting factor in the measurement of the sorption isotherm is the maximum test chamber relative humidity, which is reached when condensation forms within the system. The condensation of water vapor occurs at points in the system which are below the dew point of the test chamber air, causing relative humidity fluctuations in the chamber and unreliable measurements. In order to maximize the operational range, all parts of the system should be as close to the test chamber temperature set point as possible.

For the current apparatus, the location of the lowest temperature in the system depends upon whether the temperature set point is above or below ambient temperature. If the test chamber is at or below room temperature, then the point of lowest temperature in the system is the concentric tube counterflow heat exchanger surface temperature at the air exit. This temperature can be set within few tenths of a Celsius degree of the desired test chamber temperature, so the maximum relative humidity is very high for low temperatures. If the test chamber temperature set point is above room temperature, then the point of lowest temperature in the system is in the humidity control section. The flow control valve cannot be completely insulated, and the desiccant and distilled water are at room temperature. These conditions cause a slightly lower maximum relative humidity at high temperatures.

In practice, the maximum relative humidity reached in the 55 C experiment was not caused by the limitation described above. The limitation was caused by a procedural

problem rather than a problem with temperatures in the apparatus. At 40 per cent relative humidity, condensation formed on the inside surface of the test chamber when the chamber was opened for data collection. A new procedure for data collection at high temperatures would be required to increase the range of the current apparatus.

Moisture Content Results

Sorption isotherms for the three test materials were determined at three temperatures within the operating relative humidity range of the apparatus. The results are compared to consistent qualitative data from a reference which covers the entire humidity range and temperature range of this experiment. The reference is the table entitled "Moisture Content of Wood in Equilibrium with Stated Dry-Bulb Temperature and Relative Humidity" (Forest Products Laboratory, 1974). Although the figures in the table are just typical moisture contents for unspecified softwoods, the table is used as a general reference to compare trends in the data with temperature.

The averaged sorption isotherms of the two specimens of each material are presented in Figs. 18 through 26 . The data for these graphs are shown in Tables A-1 through A-6, in Appendix A. Also in this section, scanning results are analyzed and the variation of the sorption isotherms with temperature is investigated.

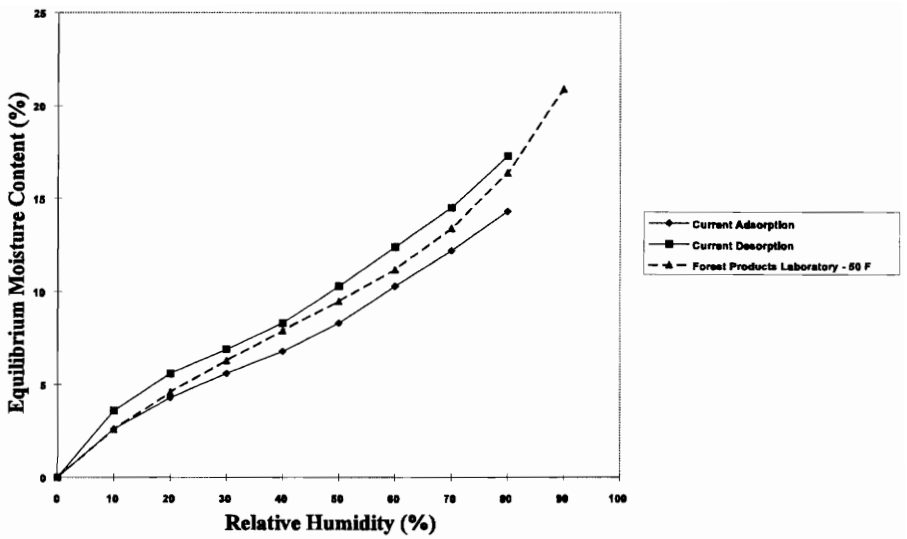

Figure 18. Sorption isotherm for EGS at 12 C.

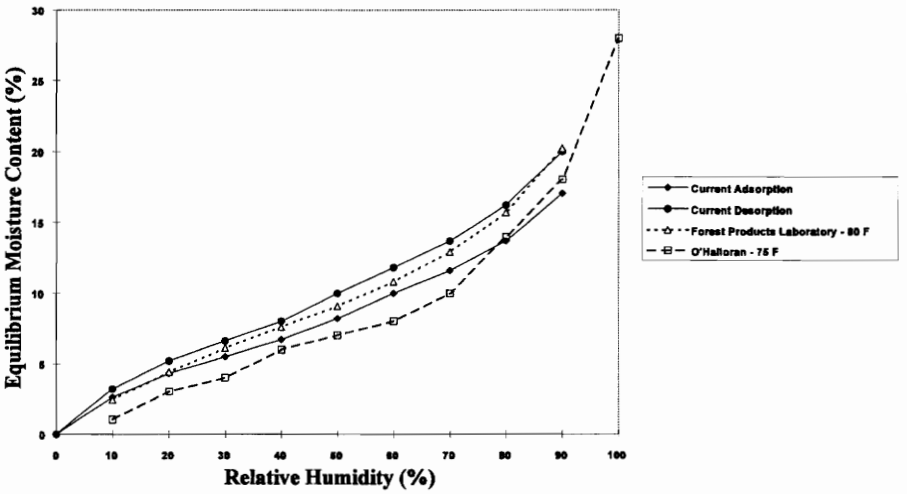

Figure 19. Sorption isotherm for EGS at 25 C.

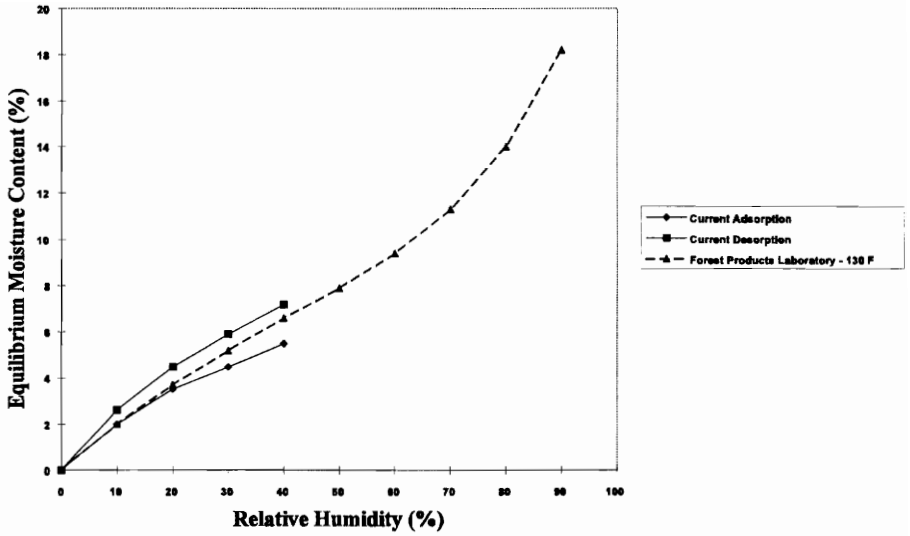

Figure 20. Sorption isotherm for EGS at 55 C.

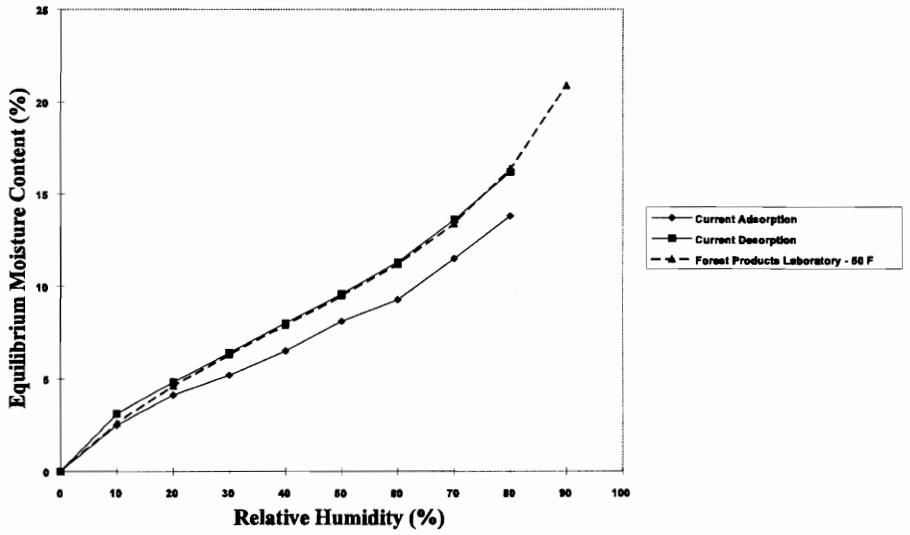

Figure 21. Sorption isotherm for OSB at 12 C.

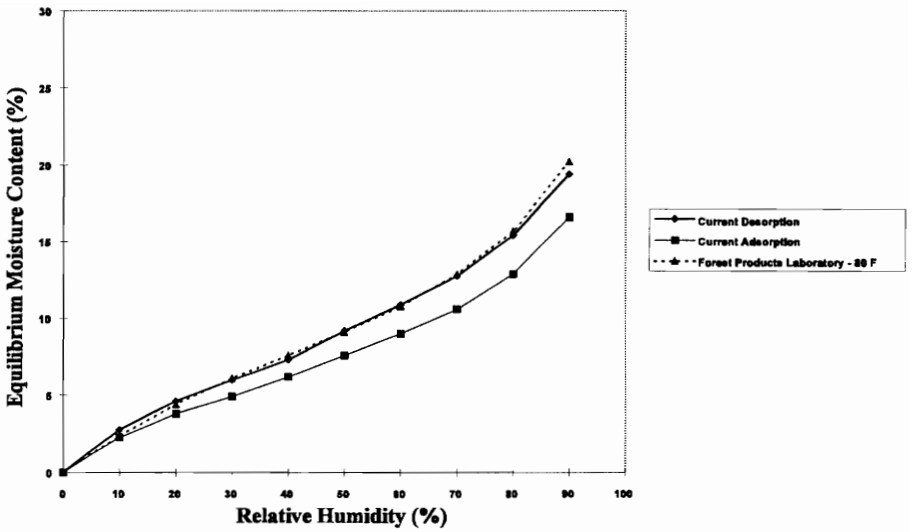

Figure 22. Sorption isotherm for OSB at 25 C.

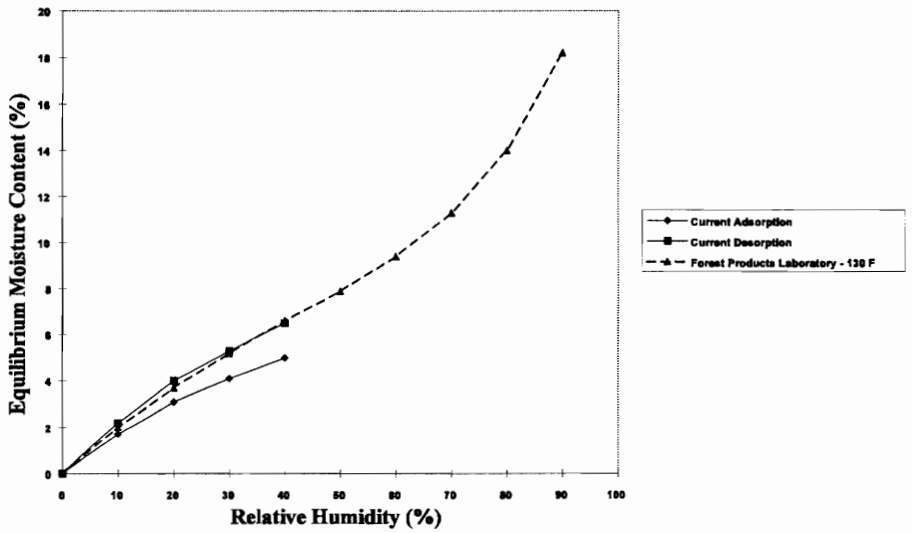

Figure 23. Sorption isotherm for OSB at 55 C.

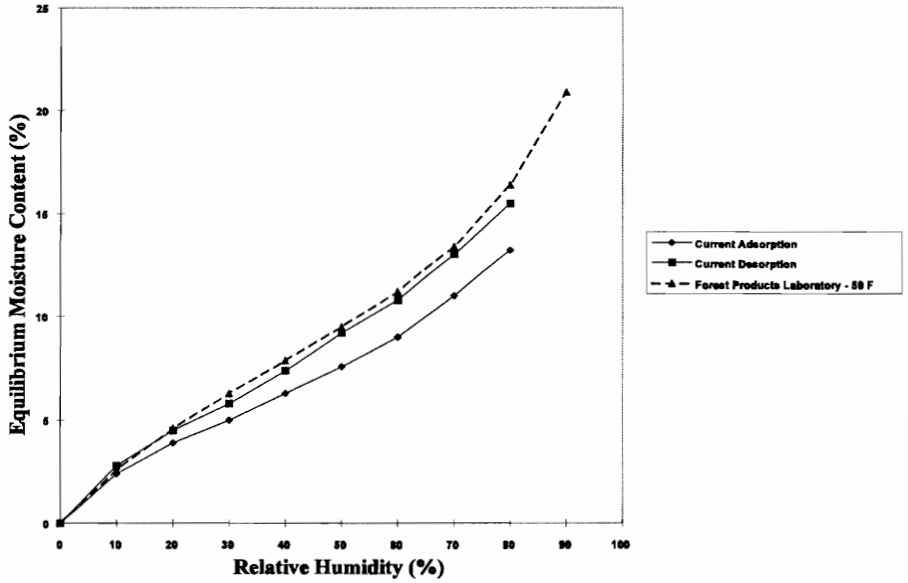

Figure 24. Sorption isotherm for FBS at 12 C.

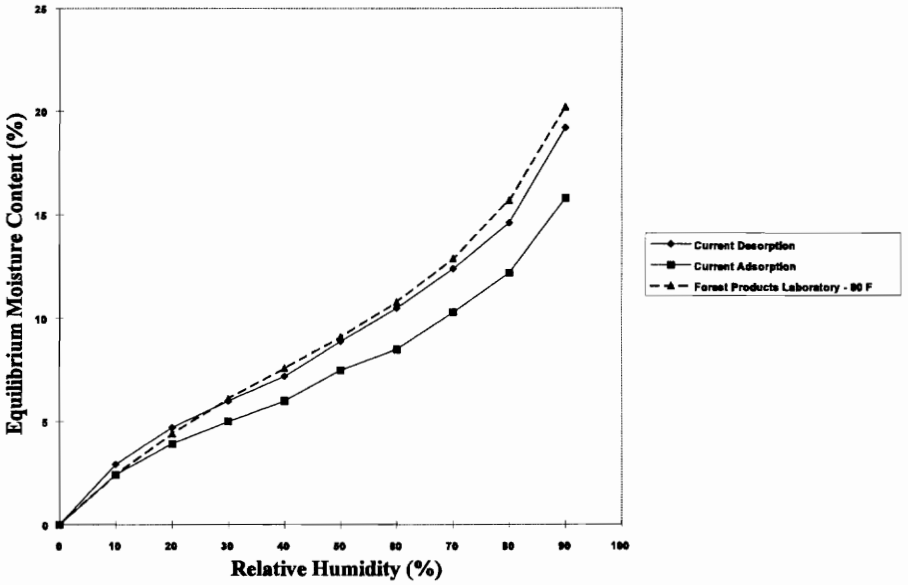

Figure 25. Sorption isotherm for FBS at 25 C.

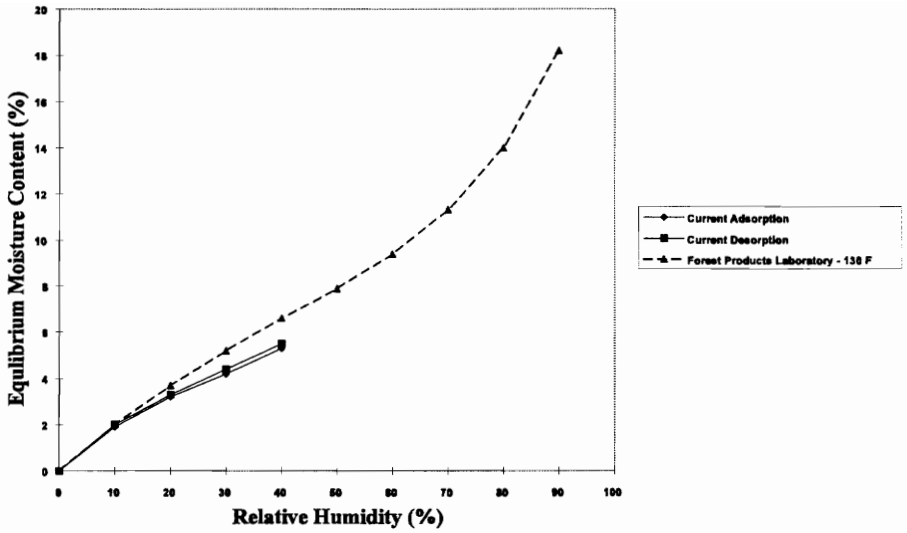

Figure 26. Sorption isotherm for FBS at 55 C.

Discussion of sorption isotherm results. The only direct comparison between the current data and Peters' previous experiment is the sorption isotherm for exterior grade plywood at 25 C. Peters actually used 20.8 C as the temperature set point, but a 4 C difference in temperature set point does not result in a significant change in sorption data (Kelsey,1957). The sorption isotherm created by Peters shows significantly higher moisture contents than the present data. This difference, however, was expected, since Peters' specimens were cut with a microtome. The plywood fell apart, which may have eliminated the effect of the adhesive between the sheets in the plywood, causing Peters'

isotherm to be closer to that of pure Douglas fir, as reported by Hedlin (1967). Because of this effect, his moisture content measurements were much higher than the data of Richards, et al. (1992), which were measured from the same sheet of plywood. The current data agree more closely with Richards, et al. Peters explained the difference as caused by Richards' higher "dry" humidity (1.4%) and the large step sizes in relative humidity in that experiment. These factors would not have as large an effect as Peters claims, however, as shown by the comparison of his data with Richards' data for the other two materials that he tested. Unfortunately, the current data do not agree closely with Peters' data for the only common temperature in the experiments, but the current data do account for a more representative test sample.

The standard reference used for all of the sorption isotherms shows the trends in the data to be consistent. The relationship between the sorption isotherm of each material and that for softwood from the FPL table is consistent for each temperature. The only exception to this trend is the 55 C isotherm for fiber board sheathing, which displayed very little hysteresis effect. There are no data in the literature for fiber board sheathing at elevated temperatures, so further investigation will be necessary to explain the observed trend.

The hysteresis effect has been reported to decrease at elevated temperatures (Skaar, 1988). However, only fiber board sheathing shows a increase in its adsorption to desorption ratio in its 55 C isotherm. This ratio is a useful parameter for determining the

extent to which hysteresis occurs in the isotherm. In terms of the adsorption to desorption ratio, fiber board sheathing shows a more narrow hysteresis band at both temperature extremes, while the hysteresis bands of oriented strand board and exterior grade plywood were slightly increased compared with their 25 C isotherms. The results do not show a conclusive trend in the hysteresis band with respect to temperature. The data points in the 55 C isotherm of fiber board sheathing are the only only points outside the expected range of 0.7 to 0.9 (as detailed in Appendix C).

The relationship between the data appears to be related to the density of the samples. Oriented strand board and fiber board sheathing have low densities, and their moisture contents tend to be less than that of plywood. This observation is surprising, since dense wood has less total space in its lumens to store moisture (Findlay, 1975). However, sorption data for these three materials at room temperature is consistent with other current results (International Energy Agency, 1996).

Exact duplication of sorption isotherm results is not meaningful, since different experimental methods result in different moisture content data. For this reason, only general comparisons have been made between the present data and data from the literature. To illustrate the variability of data, however, Fig. 27 shows the results of two independent adsorption isotherm curves for exterior grade plywood around room temperature (20-25C) (International Energy Agency, 1996) compared with the present data. This figure illustrates the effect that the variability in test procedures can produce. Biological

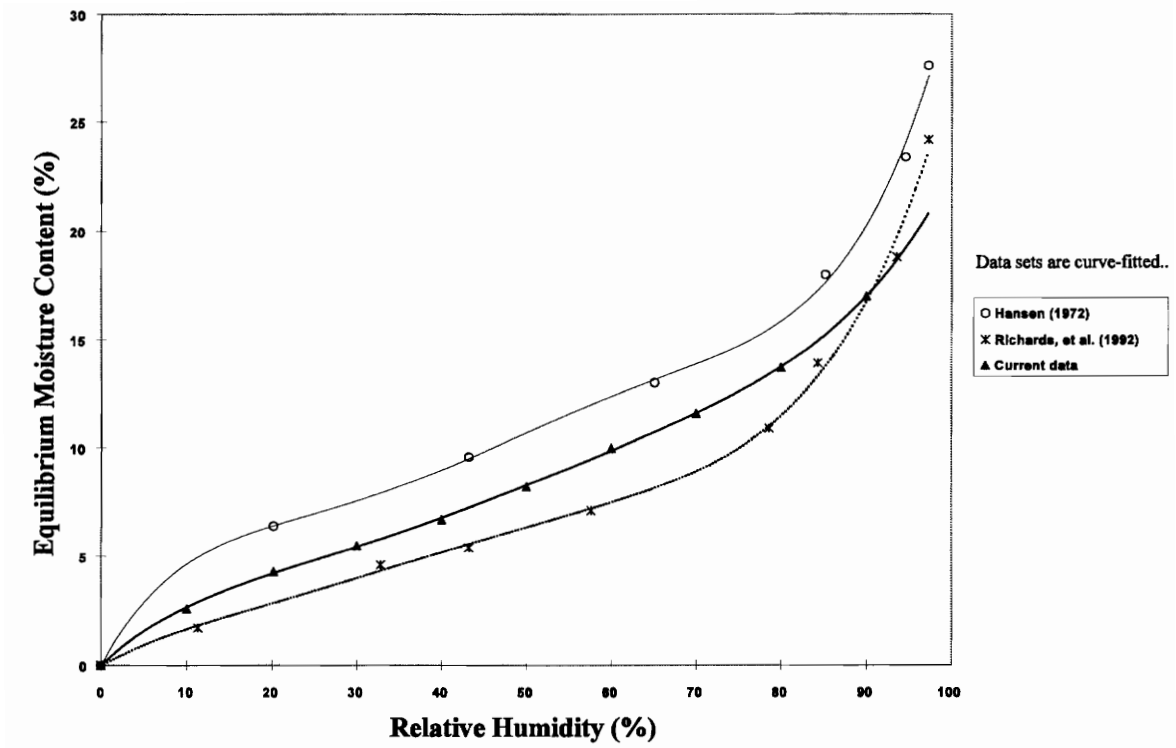

Figure 27. Comparison of current 25 C EGS adsorption curve with exisiting data.

differences can account for some inconsistency, but this effect is not strong below the fiber saturation point (Plumb, et al., 1984).

Using various methods to produce the same result is vital in assuring the accuracy of accepted data, but some standardization is required to minimize the number of variables. Some examples of factors which could be standardized are the minimum size of test specimens and the size of the step changes in relative humidity. Both of these factors can have a measurable effect upon the equilibrium moisture content of a sample. Until a sufficient amount of variables are removed from the various test procedures, the validity of different methods will be difficult to determine.

Analysis of scanning data. Two scanning curves were measured for each of the three test materials at 25 C. The measured equilibrium moisture contents of the scanning cuves are in Tables A-7 and A-8, while graphs of the curves and their relationships to their respective sorption isotherms are shown in Figs. 28 through 30. Each of the curves begins at the 50 per cent relative humidity set point on one boundary of the sorption isotherm and extends toward the other boundary. The asymptotic approach to the opposing boundary that the current scanning curves display agrees with sorption theory (Skaar, 1988). Scanning data is not commonly found in the literature.

Peters compared his scanning curve with an analytical model attributed to Pederson (1990). Pederson's scanning curve approximation is:

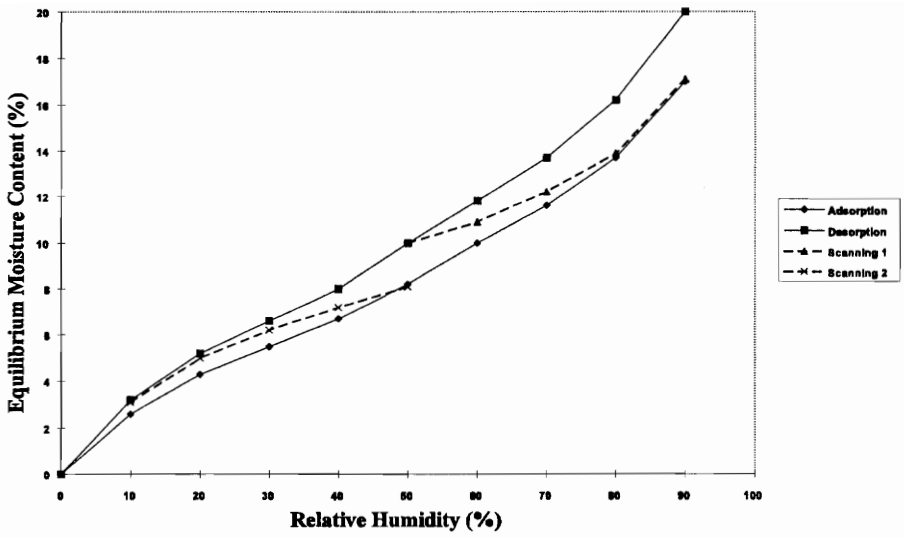

Figure 28. Sorption isotherm with scanning curves for EGS at 25 C.

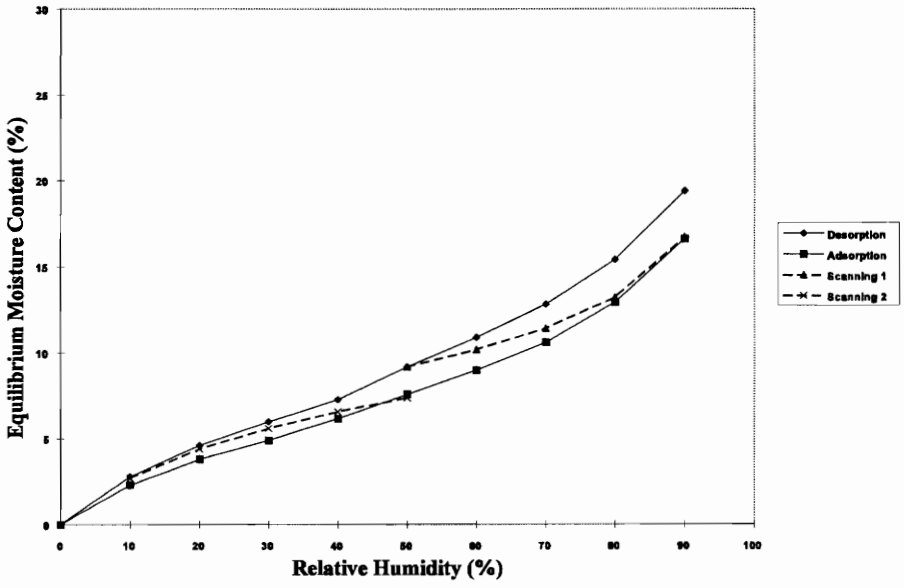

Figure 29. Sorption isotherm with scanning curves for OSB at 25 C.

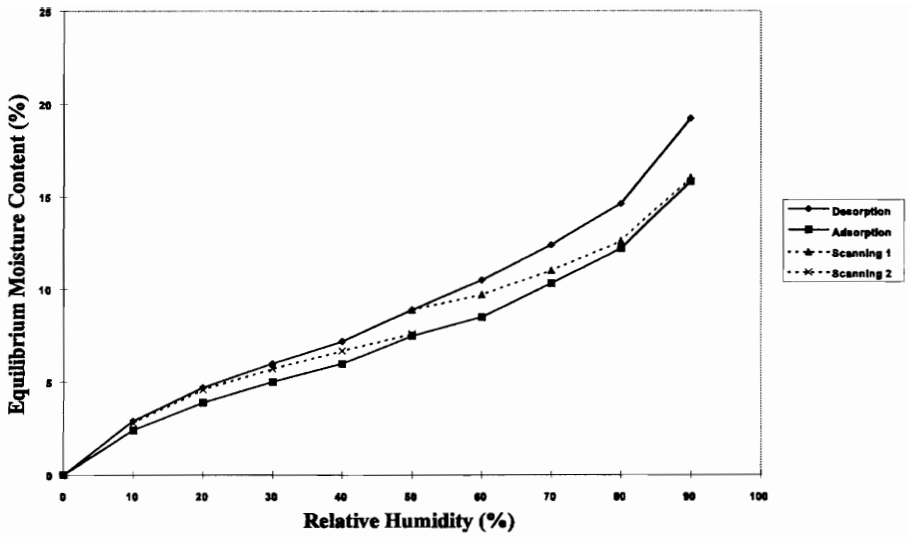

Figure 30. Sorption isotherm with scanning curves for FBS at 25 C.

$$\frac{d\gamma}{d\phi} = \frac{(\gamma - \gamma_a)^2 \frac{d\gamma_d}{d\phi} + 0.1\,(\gamma - \gamma_d)^2 \frac{d\gamma_a}{d\phi}}{(\gamma_d - \gamma_a)^2}$$

for a scanning curve from the adsorption curve to the desorption curve. Using a finite-difference approximation, Pederson's equation reduces to

$$\frac{d\gamma}{d\phi} = 0.1 \frac{d\gamma_a}{d\phi}$$

for the point on the adsorption curve, which is the initial slope for the calculated scanning curve. Peters noted that this initial slope was much less than the initial slope in his

scanning curve. If the 0.1 in Pederson's approximation is changed to 0.75, the resulting curve agrees much more closely with the current experimental data, as well as with Peters' and Peralta's results. However, the agreement of the modified Pederson's equation is still not perfect. Representative comparisons of the modified and original Pederson's approximations with experimental scanning results are shown in Figs. 31 and 32. Comparisons with the results of Peters, Peralta, and the current experiment are shown in tabular form in Appendix D.

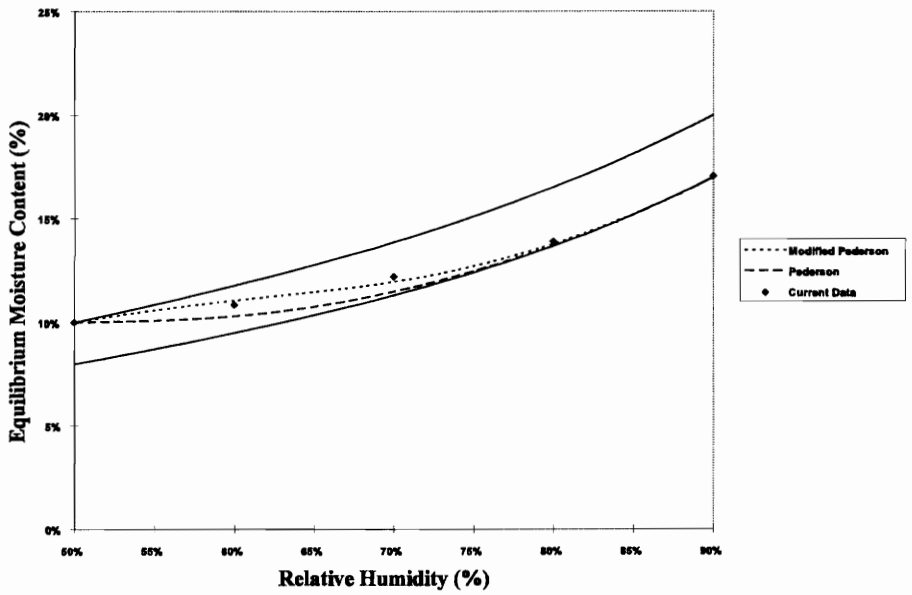

Figure 31. Comparison of Pederson's approximation with current EGS desorption-to-adsorption scanning data.

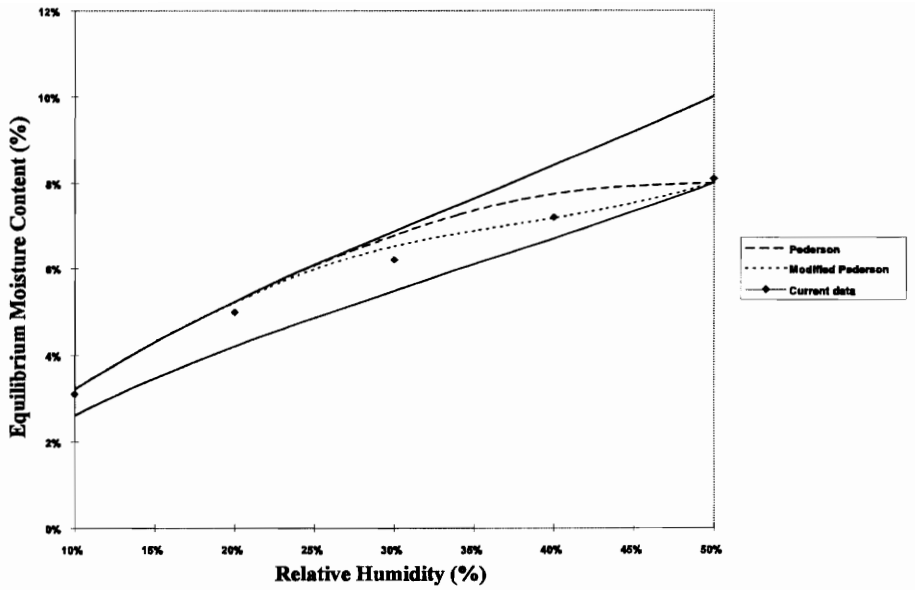

Figure 32. Comparison of Pederson's approximation with current EGS adsorption-to-desorption scanning data.

Analysis of temperature effect. Avramadis and Siau (1987) noted that higher temperatures tend to reduce the equilibrium moisture content of a material. As expected, the moisture contents at a given relative humidity varied inversely with temperature. In Figs. 31 through 33, the average of the adsorption curve and desorption curve at each relative humidity is taken as the "sorption" isotherm. The temperature is shown in the three figures for the three test materials. As expected, the moisture contents vary inversely with temperature.

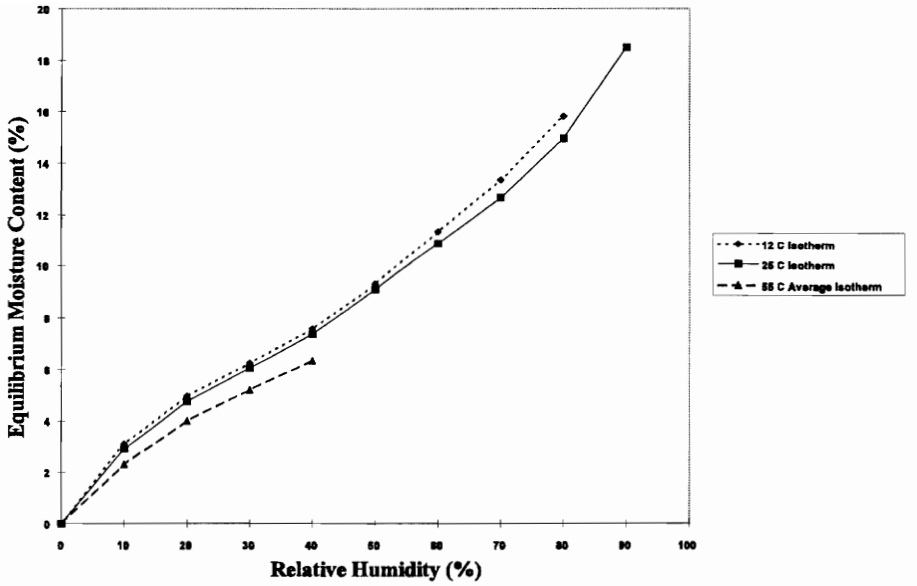

Figure 33. Variation of the average sorption isotherm of EGS with temperature.

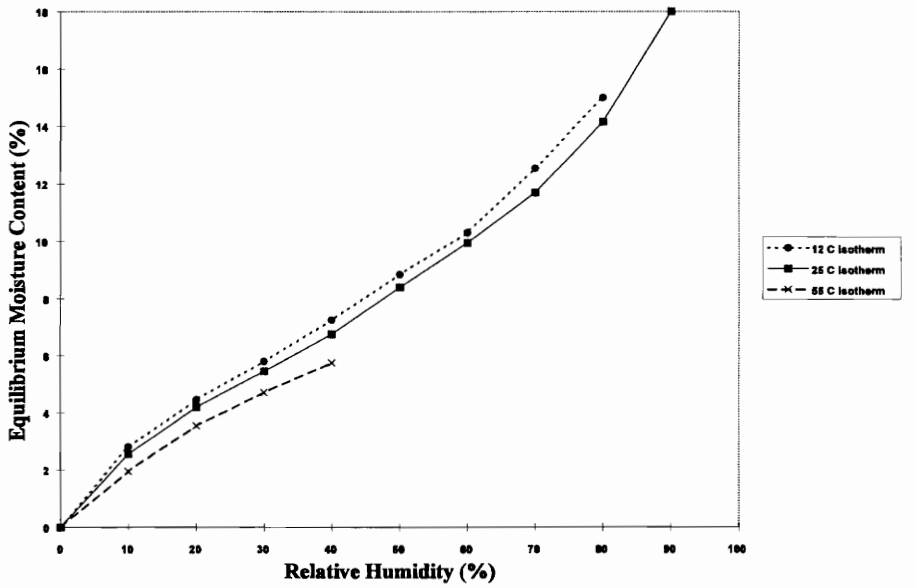

Figure 34. Variation of the average sorption isotherm of OSB with temperature.

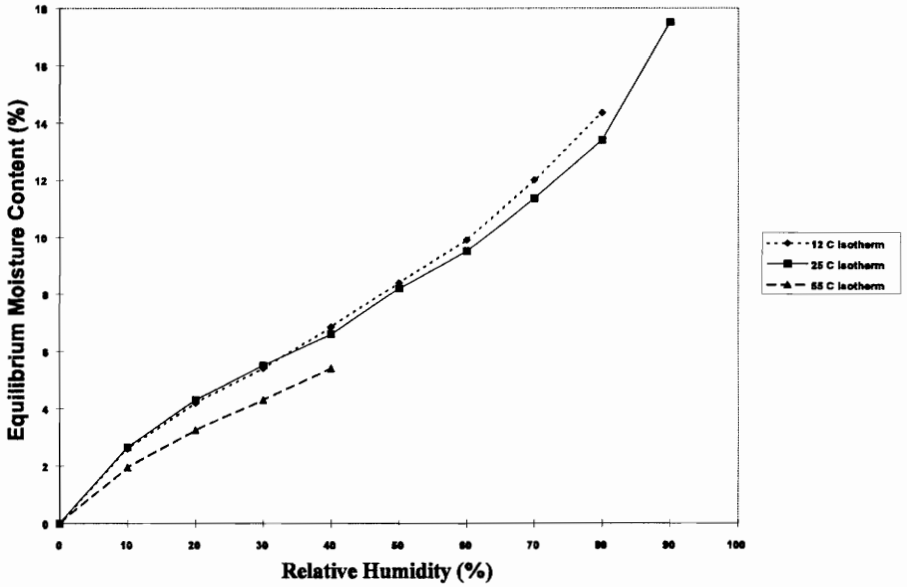

Figure 35. Variation of the average sorption isotherm of FBS with temperature.

Results Summary

One objective of the current research was to extend the range and control of the existing experimental apparatus, which was shown to be useful for determination of sorption isotherms at room temperature. The current apparatus was shown to have better stability and a wider humidity range than the previous apparatus, and the temperature limitations were explored. Sorption isotherm and scanning data were achieved quickly and

followed expected trends.

Measurement of moisture content data over a wide relative humidity and temperature range was another goal of the experiment. This goal was accomplished by measuring sorption isotherms for temperatures between 12 C and 55 C for as wide a relative humidity as possible. This process successfully produced meaningful data and uncovered limitations of the current apparatus and procedure.

Recommendations for Future Research. The experimental apparatus is currently capable of producing sorption isotherm data quickly and accurately at temperatures between 10 and 35 C over a relative humidity range of 0 to 80 per cent. Significant changes in the experimental procedure are necessary in order to increase the maximum relative humidity at temperatures above 35 C. The focus of these changes must be the further minimization of the exposure of the chamber to ambient air. Implementing a method of weighing samples without opening the test chamber, such as by placing the scale inside the test chamber, would be one solution. Another possibility would using an electrode to determine the moisture content by measuring the thermal conductivity of the sample, which would allow the control program to monitor the samples just as it monitors the relative humidity and temperature. Lowering the minimum operational temperature of the system could be effected by using instruments and tubing which are better insulated or by maintaining the contents of the bubble and desiccant tubes at the test chamber temperature.

Future research can be directed both toward increasing the range of the apparatus and toward rapid production of sorption data for many different materials within the current temperature range. Sorption data can be produced in an attempt to determine the important parameters necessary for standardization of a test method. Examples of parameters that could be tested include sample size and the size of relative humidity step changes. Sorption isotherms and scanning data are also still necessary to aid in the development of accurate models of moisture transfer in porous materials. Effects of additives and coatings can also be investigated, as well as the effect of biological differences between samples.

CONCLUSIONS

The operational capabilities of the existing experimental apparatus and measurement procedure have been further investigated. The operating range and stability were improved. The experiment involves in situ mass measurements of specimens within an environmental chamber. Conditions in the environmental chamber are controlled by a computer algorithm in conjunction with an external forced-air system.

The environmental chamber is capable of maintaining relative humidities between 0 and 90 per cent at 25 C, with control to within $\pm$ 0.3 per cent relative humidity and $\pm$ 0.1 C. The minimum test temperature is limited to approximately 10 C, because of the difficulty in insulating some of the irregularly shaped instruments and fittings in the system. The maximum temperature attainable is greater than 55 C, but the relative humidity ceiling at high temperatures is limited. A significant change must be implemented in order to increase the maximum relative humidity at high temperatures.

Some suggestions for such a change are the creation of an environmental chamber around the test chamber or measuring moisture contents with an electrode. A second environmental chamber would eliminate the sharp temperature and relative humidity

gradients at the opening of the test chamber. Moisture contents can also be determined from the thermal conductivities of the samples. Another possibility would be to heat the top surface of the test chamber before it is opened. The primary concern for a solution is condensation formed by the contact between ambient air and test chamber air when the access plug is removed for data collection.

Sorption isotherms were measured within the limits of the apparatus for exterior grade plywood, oriented strand board, and fiber board sheathing at temperatures of 12 C, 25 C and 55 C. The equilibrium moisture contents for each material varied inversely with temperature. The ratio of the adsorption moisture contents to the desorption contents was investigated, and the results were inconclusive. For the 25 C isotherms, scanning curves were created starting from the 50 per cent relative humidity set point on the adsorption and desorption curves. All of the observed trends of the current data are in qualitative agreement with the few available sources of moisture content data for wood-based materials. .

REFERENCES

Peters, R. E., 1992, "An Experimental Apparatus for the Measurement of Sorption Isotherms of Moisture in Porous Building Materials", M.S. Thesis, Virginia Polytechnic Institute and State University, Blacksburg, Virginia.

Thomas, W. C. and D. M. Burch, 1990, "Experimental Validation of a Mathematical Model for Predicting Water Vapor Sorption at Interior Building Surfaces", ASHRAE Transactions, Vol. 96, Pt. 1, pp 487-496.

Kumaran, M. K., 1990, "Application of Gamma-Ray Spectroscopy for Determination of Moisture Distribution in Insulating Materials", Heat and Mass Transfer in Building Materials and Structures, Hemisphere Publishing Corporation, New York, pp 95-103.

Burch, D. M. and W. C. Thomas, 1991, "Analysis of Moisture Accumulation in a Wood-Frame Cavity Wall Subjected to Winter Climate", National Institute of Standards and Technology Interim Report 4674, U.S. Department of Commerce, NIST, Gaithersburg, MD.

Krus, M., 1992, "Does Water Vapor Diffusion Really Depend on Moisture Content?", Proceedings of the International Energy Agency Annex 24, Saskatoon, Canada.

Wadsö, Lars, 1994, "Unsteady-State Water Vapor Adsorption in Wood: An Experimental Study", Wood and Fiber Science, Vol. 26, No. 1.

Peralta, Perry N., 1995b, "Modelling Wood Moisture Sorption Hysteresis Using the Independent-Domain Theory", Wood and Fiber Science, Vol. 27, No. 3, pp 250-264.

Cunningham, M. J., 1995, "A Model to Explain 'Anomalous' Moisture Sorption in Wood Under Step Function Driving Forces", Wood and Fiber Science, Vol. 27, No. 3, pp 265-277.

Peralta, Perry N., 1995a, "Moisture Sorption Within a Limited RH Range", Wood and Fiber Science, Vol. 27, No. 1.

Forest Products Laboratory, 1974, Wood Handbook: Wood as an Engineering Material, Agriculture Handbook No. 72, U.S. Department of Agriculture Forest Service, U.S. Government Printing Office, Washington, DC.

Findlay, W. P. K., 1975, Timber: Its Properties and Uses, Granada Publishing, New York.

Brunauer, S., 1943, The Adsorption of Gases and Vapors, Princeton University Press, Princeton, NJ.

Van Wylen, Gordon J. and Richard E. Sonntag, 1943, Fundamentals of Classical Thermodynamics, John Wiley and Sons, New York.

Okoh, K. I. A. and C. Skaar, 1980, "Moisture Sorption Isotherms of the Wood and Inner Bark of Ten Southern U.S. Hardwoods", Wood and Fiber Science, Vol. 12, No.12, pp 98-111.

Luikov, A. V. and Y. A. Mikhailov, 1961, Theory of Energy and Mass Transfer, Prentice Hall, New York.

Gui, Young Q., E. William Jones, Fred W. Taylor and Camille A. Issa, 1994, "An Application of Finite Element Analysis to Wood Drying", Wood and Fiber Science, Vol. 26, No. 2, pp 281-293.

Fick, Adolph, 1855, "On Liquid Diffusion", Philosophical Magazine X, Proceedings of the Royal Society of London.

Chevrier, V. F., 1996, "Moisture Transfer in Porous Materials Exposed to Combined Humidity and Temperature Gradients", M.S. Thesis, Virginia Polytechnic Institute and State University, Blacksburg, VA.

Whitaker, Stephen, 1986, "Flow in Porous Media II: The Governing Equations for Immiscible, Two-Phase Flow", Transport in Porous Media I, pp 105-125.

Berger, D. and D. C. T. Pei, 1973, "Drying of Hygroscopic Capillary Porous Solids-A Theoretical Approach", International Journal of Mass Transfer, Vol. 16, pp 293-302.

Leung, Henry K., 1986, "Water Activity and Other Colligative Properties of Foods", Physical and Chemical Properties of Food, American Society of Agricultural Engineers, St. Joseph, MI.

Fortes, M. and Martin R. Okos, 1980, Advances in Drying, Hemisphere Publishing, Washington, DC, Vol. 1, Chapter 5.

Rosen, Howard N., 1987, "Recent Advances in the Drying of Wood", Advances in Drying, Vol. 4, Hemisphere Publishing Co., Washington, DC.

Babbitt, J. D., 1950, "On the Differential Equations of Diffusion", Canadian Journal of Research, Section A, Vol. 18, pp 419-474.

Spolek, G. A. and O. A. Plumb, 1980, "A Numerical Model of Heat and Mass Transport in Wood During Drying", Drying '80, Hemisphere Publishing, Washington, DC, pp 84-92.

Ferguson, W. J. and R. W. Lewis, 1993, "A Fully Nonlinear Analysis of Temperature, Moisture Content, and Pressure in a Capillary Porous Body", Numerical Heat Transfer, Part B, Vol. 23, pp 91-110.

Hedlin, C. P., 1967, "Sorption Isotherms of Twelve Woods at Subfreezing Temperatures", Forest Products Journal, Vol. 17, No. 12, pp 43-48.

Kumaran, M. K., 1988, "Comparison of Simultaneous Heat and Moisture Transport Through Glass-Fiber and Spray-Cellulose Insulations", Journal of Thermal Insulation, Vol. 12, pp 6-16.

Kohonen, Reijo, 1984, "A Method to Analyze the Transient Hygrothermal Behavior of Building Materials and Components", Publication 21, Technical Research Center of Finland.

International Energy Agency, 1990, Energy Conservation in Building and Community Systems Guidelines and Practice, Vol. 2, IEA Annex XIV.

Powell, R. L., W. J. Hall, C. H. Hyink, Jr., L. L. Sparks, G. W. Burns, M. G. Scroger and H.H. Plumb, 1974, "Thermocouple Reference Tables Based on the IPTS-68", NBS Monograph 125, U.S. Department of Commerce.

Stamm, A. J., 1964, Wood and Cellulose Science, The Ronald Press Company, New York.

Coudon, C. R., 1994, "Moisture in Building Materials", Undergraduate Research Project, Virginia Polytechnic Institute and State University, Blacksburg, VA.

Goff, J. A. and S. Gratch, 1946, "Low-pressure Properties of Water from -160 to 212 F", ASHVE Transactions, Vol. 52, pp 95-122.

Smith, Carlos A. and A. B. Corripio, 1985, Principles and Practice of Automatic Process Control, John Wiley and Sons, New York, Chapter 5.

Richards, R. F., D. M. Burch and W. C. Thomas, 1992, "Water Vapor Sorption Measurements of Building Materials", ASHRAE Transactions, Vol. 98, Pt. 2.

Christensen, G. N., 1960, "Kinetics of Sorption of Water Vapor in Wood: Effect of Sample Thickness", Australian Journal of Applied Science, Vol. 11, No. 2, pp 295-304.

Simpson, William T., John L. Tschernitz and James S. Serfo, 1994, "Short Clear Specimens for Estimating Drying Time of Sugar Maple Lumber", Wood and Fiber Science, Vol. 26, No. 2, pp 171-184.

Kelsey, K. E., 1957, "The Sorption of Water Vapor by Wood", Australian Journal of Applied Science, Vol. 8, No. 1, pp 42-54.

O'Halloran, M. R., 1975, "Plywood in Hostile Environments", Research Report 132, American Plywood Association Technical Services Division, Tacoma, WA.

International Energy Agency, 1996, Heat, Air and Moisture Transfer in Insulated Envelope Parts, Vol. 3, Laboratorium Bouwfysica, K.U.-Leuven, Belgium.

Plumb, O. A., C. A. Brown and B. A. Olmstead, 1984, "Experimental Measurement of Heat and Mass Transfer During Convective Drying of Southern Pine", Wood Science and Technology, Springer-Verlag, New York.

Skaar, Christen, 1988, Wood-Water Relations, Springer-Verlag, New York.

Pederson, C. R., 1990, "Combined Heat and Moisture Transfer in Building Constructions", Ph.D. Dissertation, Thermal Insulation Laboratory, Technical University of Denmark.

Avramadis, S. and J. F. Siau, 1987, "An Investigation of the External and Internal Resistance to Moisture Diffusion in Wood", Wood Science and Technology, Vol. 1, No. 3, pp 249-256.

APPENDIX A

Equilibrium Moisture Content Data

The following tables contain the current experimental data for sorption isotherms. The numbers given in the tables are moisture content expressed as a percentage of the dry mass of the sample.

Table A-1. Equilibrium moisture content adsorption data for all test specimens at 25 C.

RH Set Pt	EGS 1	EGS 2	OSB 1	OSB 2	FBS 1	FBS 2
0	0.0	0.0	0.0	0.0	0.0	0.0
10	2.6	2.6	2.3	2.3	2.4	2.4
20	4.3	4.3	3.8	3.8	3.9	3.9
30	5.5	5.4	4.9	4.9	5.0	4.9
40	6.7	6.6	6.2	6.2	6.0	5.9
50	8.2	8.1	7.6	7.6	7.5	7.5
60	10	9.9	9.0	9.0	8.5	8.5
70	11.6	11.6	10.6	10.7	10.3	10.2
80	13.7	13.6	12.9	12.9	12.2	12.1
90	17.0	17.0	16.6	16.7	15.8	15.7

Table A-2. Equilibrium moisture content desorption data for all test specimens at 25 C.

RH Set Pt	EGS 1	EGS 2	OSB 1	OSB 2	FBS 1	FBS 2
90	20.0	20.1	19.4	19.4	19.2	19.0
80	16.2	16.3	15.4	15.5	14.6	14.5
70	13.7	13.7	12.8	12.8	12.4	12.3
60	11.8	11.7	10.9	10.9	10.5	10.4
50	10.0	9.9	9.2	9.3	8.9	8.9
40	8.0	8.0	7.3	7.3	7.2	7.1
30	6.6	6.5	6.0	6.1	6.0	5.9
20	5.2	5.2	4.6	4.6	4.7	4.7
10	3.2	3.1	2.8	2.8	2.9	2.9
0	0.0	0.0	0.0	0.0	0.0	0.0

Table A-3. Equilibrium moisture content adsorption data for all test specimens at 12 C.

RH Set Pt	EGS 1	EGS 2	OSB 1	OSB 2	FBS 1	FBS 2
0	0.0	0.0	0.0	0.0	0.0	0.0
10	2.6	2.6	2.5	2.5	2.4	2.5
20	4.3	4.3	4.1	4.2	3.9	3.9
30	5.6	5.6	5.2	5.3	5.0	5.0
40	6.8	6.7	6.5	6.5	6.3	6.3
50	8.3	8.3	8.1	8.1	7.6	7.6
60	10.3	10.2	9.3	9.3	9.0	8.9
70	12.2	12.1	11.5	11.6	11.0	11.1
80	14.3	14.3	13.8	13.9	13.1	13.3

Table A-4. Equilibrium moisture content desorption data for all test specimens at 12 C.

RH Set Pt	EGS 1	EGS 2	OSB 1	OSB 2	FBS 1	FBS 2
80	17.3	17.2	16.2	16.2	15.5	15.6
70	14.5	14.4	13.6	13.7	13.0	13.1
60	12.4	12.3	11.3	11.3	10.8	10.9
50	10.3	10.3	9.6	9.7	9.2	9.3
40	8.3	8.2	8.0	8.1	7.4	7.5
30	6.9	6.8	6.4	6.4	5.8	5.9
20	5.6	5.5	4.8	4.8	4.5	4.5
10	3.6	3.6	3.1	3.1	2.8	2.8
0	0.0	0.0	0.0	0.0	0.0	0.0

Table A-5. Equilibrium moisture content adsorption data for all test specimens at 55 C.

RH Set Pt	EGS 1	EGS 2	OSB 1	OSB 2	FBS 1	FBS 2
0	0.0	0.0	0.0	0.0	0.0	0.0
10	2.0	2.0	1.7	1.7	1.9	1.9
20	3.5	3.5	3.1	3.1	3.2	3.2
30	4.5	4.4	4.1	4.2	4.2	4.2
40	5.5	5.4	5.0	5.0	5.3	5.3

Table A-6. Equilibrium moisture content desorption data for all test specimens at 55 C.

RH Set Pt	EGS 1	EGS 2	OSB 1	OSB 2	FBS 1	FBS 2
40	7.2	7.2	6.5	6.5	5.5	5.6
30	5.9	5.8	5.3	5.4	4.4	4.5
20	4.5	4.4	4.0	4.1	3.3	3.4
10	2.6	2.5	2.2	2.2	2.0	2.0
0	0.0	0.0	0.0	0.0	0.0	0.0

Tables A-7 and A-8 show the scanning curve data obtained in the present experiment. All values are expressed as moisture content percentage with respect to the dry mass of the sample.

Table A-7. Adsorption scanning data for all test specimens at 25 C.

RH Set Pt	EGS 1	EGS 1	OSB 1	OSB 2	FBS 1	FBS 2
50	10.0	9.9	9.2	9.2	8.9	8.9
60	10.9	10.8	10.2	10.2	9.7	9.7
70	12.2	12.2	11.4	11.5	11.0	10.9
80	13.9	13.9	13.2	13.2	12.6	12.5
90	17.1	17.0	16.7	16.8	16.0	15.8

Table A-8. Desorption scanning data for all test specimens at 25 C.

RH Set Pt	EGS 1	EGS 2	OSB 1	OSB 2	FBS 1	FBS 2
50	8.1	8.0	7.4	7.4	7.6	7.5
40	7.2	7.2	6.6	6.6	6.7	6.7
30	6.2	6.1	5.6	5.6	5.7	5.7
20	5.0	5.0	4.4	4.4	4.6	4.6
10	3.1	3.0	2.7	2.7	2.8	2.8

Appendix B - Control Program

The following is a listing of the GWBASIC program used to monitor and control the environment in the test chamber. Not shown here is the opening routine, which is copyright protected by Hewlett Packard. The purpose of the omitted section of code is to initialize the Hewlett Packard HP-IB interfaces.

```
999 REM **END PROGRAM SETUP**
1000 REM **BEGIN CONSTANTS & DIMENSIONS**
1010 REM constants for thermocouple temperature as a function voltage for -270  to 0 Celsius
1020 AC1=.02383709#
1030 AC2=-.0000029878839#
1040 AC3=-.0000000007194581#
1050 AC4=-1.0041943D-13
1060 REM constants for thermocouple temperature as a function of voltage for   0 to 400 Celsius
1070 AH1=.025661297#
1080 AH2=-.00000061954869#
1090 AH3=2.2181644D-11
1100 AH4=-3.55009D-16
1110 REM constants for converting the reference temperature to a type-T thermocouple voltage for software compensation. Temp less than 0 Celsius      (NBS monogram 125)
1120 BC1=38.74077384#
1130 BC2=.044123932482#
1140 BC3=.00011405238498#
1150 BC4=.000019974406568#
1160 BC5=9.0445401187D-07
1170 BC6=2.2766018504D-08
1180 BC7=3.624740938D-10
1190 BC8=3.8648924201D-12
1200 BC9=2.8298678519D-14
```

```
1210 BC10=1.4281383349D-16
1220 BC11=4.8833254364D-19
1230 BC12=1.0803474683D-21
1240 BC13=1.3949291026D-24
1250 BC14=7.9795893156D-28
1260 REM constants for converting the reference temperature to a type-T
thermocouple voltage for software compensation. Temp. greater than 0 Celsius (NBS
monogram 125)
1270 BH1=38.74077384#
1280 BH2=.033190198092#
1290 BH3=.00020714183645#
1300 BH4=-.0000021945834823#
1310 BH5=1.103190055D-08
1320 BH6=-3.0927581898D-11
1330 BH7=4.5653337165D-14
1340 BH8=-2.761687804D-17
1350 REM ****DIMENSIONING****
1360 DIM DEWPOINT(150),RELH(150)
1370 STEPCT=0
1375 REM ****DEV=709 IS THE LOCATION OF THE DATA ACQUISITION
UNIT****
1376 REM ****DEV2=706 IS THE LOCATION OF THE POWER SUPPLY
PROGRAMMER****
1380 DEV = 709
1390 DEV2=706
1400 REM ****INITIALIZING VARIABLES FOR THE CONTROL
SUBROUTINE****
1410 IE=0
1420 DE=0
1430 E1=0
1440 K=1
1450 TI=10
1460 TD=25
1470 N=0
1480 TK=10
1490 LOCATE 22,22: PRINT"                "
1500 REM ****CLEARING DEVICE INTERFACE****
1505 REM **AI CALLS THE DATA ACQUISITION UNIT, THE NUMBER IS THE**
1506 REM ****CHANNEL TO BE READ****
1510 RR$="AI19"
```

```
1520 TT$="AI05"
1530 V1$="AI63"
1540 V2$="AI40"
1550 CC$="AI62"
1560 G=1
1570 IT=0
1580 INPUT"PLEASE ENTER THE HUMIDITY SET POINT(0-100%): ",SETPT
1590 IF (SETPT<0) OR (SETPT>100) THEN 1450
1600 INPUT"WHAT IS THE CURRENT STEPPER MOTOR POSITION";STEPCT
1610 IF STEPCT<0 THEN 1580
1620 IF STEPCT=0 THEN 1670
1630 G=0:INPUT"IS THE B)UBBLE TUBE OR THE D)ESICCANT ON"; A$
1640 IF A$="B" THEN N=-1
1650 IF A$="D" THEN N=1
1660 IF (A$<>"B") AND (A$<>"D") THEN 1630
1670 INPUT"PLEASE ENTER THE TEMPERATURE SET POINT (0-60C): ",SETT
1680 IF (SETT<0) OR (SETT>60) THEN 1670
1690 INPUT"WHAT IS THE CURRENT POWER SUPPLY POSITION (2000-2999)";C
1700 IF (C<2000) OR (C>2999) THEN 1690
1710 CLS
1720 GOSUB 2000
1730 D=0
1740 RHV1=0
1750 RHV2=0
1760 REM **CONTINUE LOOP**
1770 GOTO 1720
1999 REM **END CONSTANTS & DIMENSIONS**
2000 REM **BEGIN MAIN PROGRAM**
2005 REM **AUTOMATIC CONTROL OF HUMIDITY**
2010 GOSUB 7000
2015 REM ****DETERMINE DIFFERENCE BETWEEN ACTUAL AND DESIRED
T & RH****
2020 E=RHV2-SETPT
2030 IF N<>0 THEN 2060
2040 GOSUB 9000
2050 GOTO 2090
2060 GOSUB 8000
2070 IF G=0 THEN 2075
2080 GOSUB 6000
2090 G=1
```

```
2100 IF ABS(E)<1 THEN COLOR 21
2110 LOCATE 6,25:PRINT"SET POINT: ";SETPT: COLOR 14,1
2120 LOCATE 9,5: PRINT C
2130 FOR I=1 TO 30000
2140 NEXT I
2150 RETURN
2999 REM **END MAIN PROGRAM**
3000 REM **BEGIN REFERENCE TEMPERATURE AMD VOLTAGE CALCULATIONS**
3010 REM ****REFERENCE VOLTAGE FOR TEMPERATURE < 0C****
3 0 2 0 V R E F =
(BC1*TR)+(BC2*(TR*TR))+(BC3*(TR^3))+(BC4*(TR^4))+(BC5*(TR^5))+(BC6*
(TR^6))+(BC7*(TR^7))+(BC8*(TR^8))+(BC9*(TR^9))+(BC10*(TR^10))+(BC11*(
TR^11))+(BC12*(TR^12))+(BC13*(TR^13))+(BC14*(TR^14))
3030 RETURN
3100 REM ****REFERENCE VOLTAGE FOR TEMPERATURE > 0C****
3 1 1 0 V R E F =
(BH1*TR)+(BH2*(TR*TR))+(BH3*(TR^3))+(BH4*(TR^4))+(BH5*(TR^5))+(BH6
*(TR^6))+(BH7*(TR^7))+(BH8*(TR^8))
3120 RETURN
3999 REM **END REFERENCE TEMPERATURE AND VOLTAGE CALCULATIONS**
4000 REM **BEGIN NEWTON-RAPHSON TEMPERATURE CALCULATION**
4005 REM ****USING THE THERMOCOUPLE CONSTANTS DEFINED FOR T < 0C****
4010 T0=(AC1*V)+(AC2*(V^2))+(AC3*(V^3))+(AC4*(V^4))
4020 T1=T0
4 0 3
V1=BC1*T1+BC2*T1^2+BC3*T1^3+BC4*T1^4+BC5*T1^5+BC6*T1^6+BC7*
T1^7+BC8*T1^8
4 0 4
V1=V1+BC9*T1^9+BC10*T1^10+BC11*T1^11+BC12*T1^12+BC13*T1^13+B
C14*T1^14
4 0 5
DV1=BC1+2*BC2*T1+3*BC3*T1^2+4*BC4*T1^3+5*BC5*T1^4+6*BC6*T1^5
+7*BC7*T1^6
4 0 6
DV1=DV1+8*BC8*T1^7+9*BC9*T1^8+10*BC10*T1^9+11*BC11*T1^10+12*B
C12*T1^11
4070 DV1=DV1+13*BC13*T1^12+14*BC14*T1^13
```

```
4080 C1=V1-V
4090 TEMP5 = T2
4100 T2=T1-(C1/DV1)
4                    1                    1
V2=BC1*T2+BC2*T2^2+BC3*T2^3+BC4*T2^4+BC5*T2^5+BC6*T2^6+BC7*
T2^7+BC8*T2^8
4                    1                    2
V2=V2+BC9*T2^9+BC10*T2^10+BC11*T2^11+BC12*T2^12+BC13*T2^13+B
C14*T2^14
4                    1                    3
DV2=BC1+2*BC2*T2+3*BC3*T2^2+4*BC4*T2^3+5*BC5*T2^4+6*BC6*T2^5
+7*BC7*T2^6
4                    1                    4
DV2=DV2+8*BC8*T2^7+9*BC9*T2^8+10*BC10*T2^9+11*BC11*T2^10+12*B
C12*T2^11
4150 DV2=DV2+13*BC13*T2^12+14*BC14*T2^13
4160 C2=V2-V
4170 EE = C2/V
4180 IF ABS(EE) <=.000001 THEN 4660
4190 T1=T2
4200 GOTO 4030
4500 REM **USING THE THERMOCOUPLES DEFINED FOR T > 0C**
4510 T0= (AH1*V)+(AH2*(V^2))+(AH3*(V^3))+(AH4*(V^4))
4520 T1=T0
4                    5                    3
V1=BH1*T1+BH2*T1^2+BH3*T1^3+BH4*T1^4+BH5*T1^5+BH6*T1^6+BH7*
T1^7+BH8*T1^8
4                    5                    4
DV1=BH1+2*BH2*T1+3*BH3*T1^2+4*BH4*T1^3+5*BH5*T1^4+6*BH6*T1^5
+7*BH7*T1^6
4550 DV1=DV1+8*BH8*T1^7
4560 C1=V1-V
4570 T2=T1-(C1/DV1)
4580V2 =BH1*T2 + BH2*T2^2 + BH3*T2^3 + BH4*T2^4 + BH5*T2^5 + BH6*
T2^6 + BH7*T2^7 + BH8*T2^8
4590 DV2=BH1 + 2*BH2*T2 + 3*BH3*T2^2 + 4*BH4*T2^3 + 5*BH5*T2^4 +
6*BH6*T2^5 + 7*BH7*T2^6
4600 DV2=DV2+8*BH8*T2^7
4610 C2=V2-V
4620 EE = C2/V
```

```
4630 IF ABS(EE) <=.000001 THEN 4660
4640 T1=T2
4650 GOTO 4530
4660 TEMP5 = T2
4670 RETURN
4999 REM **END NEWTON-RAPHSON TEMPERATURE CALCULATION**
5000 REM **BEGIN VAPOR PRESSURE CALCULATION**
5010 T1=T0
5020 X=373.16#/(T+273.16#)
5030 IF (T <= 0) THEN GOTO 5100
5040 REM ****CALCULATION FOR TEMPERATURE > 0C****
5050 PWLOG=5.02808#*LOG(X)/LOG(10#) - .00000013816#* (10#^ (11.334# * (1#-
(1#/X) ))-1#)
5060 PWLOG1=PWLOG-7.90298#*(X-1#)+.0081328#*(10#^(-3.49149#*(X-1#))-1#)
5070 PWLOG2=PWLOG1+LOG(101324.6#)/LOG(10#)
5080 PSAT=10#^PWLOG2
5090 RETURN
5100 REM ****CALCULATION FOR TEMPERATURE <0C****
5110 PILOG=-9.09718#*(X-1#)-3.56654#*LOG(X)/LOG(10#)+.876793#*(1#-(1#/X))
5120 PILOG1=PILOG+LOG(610.71#)/LOG(10#)
5130 PSAT=10#^PILOG1
5140 RETURN
5999 REM **END VAPOR PRESSURE CALCULATION**
6000 REM **BEGIN STEPPER MOTOR CONTROL**
6010 REM ****STEPPER MOTOR ROUTINE****
6020 PA=736:PB=740:PC=744:CO=748
6030 OUT CO,192
6040 OUT PC,5
6050 MODEAB=2^5
6060 MODECD=2^7   'HALF STEP
6070 REM ********
6080 ENABLE=1+2+4+8
6090 PORTB=MODECD+ENABLE+MODEAB
6100 OUT PB,PORTB
6110 DISABLE=2+4+8
6120 PORTB=DISABLE+MODECD+MODEAB
6130 OUT PB,PORTB
6140 FOR J=1 TO NS
6150 IF STEPCT=3500 THEN 6240
6160 IF DIR=0 THEN STEPCT=STEPCT+1
```

```
6170 IF STEPCT=0 THEN 6240
6180 IF DIR=1 THEN STEPCT=STEPCT-1
6190 IF DIR=0 THEN OUT PA,1
6200 IF DIR=0 THEN OUT PA,0
6210 IF DIR=1 THEN OUT PA,17
6220 IF DIR=1 THEN OUT PA,16
6230 LOCATE 13,5:PRINT"STEPPER MOTOR OPEN ";STEPCT;" CLICKS"
6240 NEXT J
6250 IF STEPCT=0 THEN N=0
6260 IF STEPCT=3500 THEN STEPCT=STEPCT-1
6270 PORTB=MODECD+ENABLE+MODEAB
6280 OUT PB,PORTB
6290 RETURN
6999 REM **END STEPPER MOTOR CONTROL**
7000 REM **BEGIN READINGS AND CALCULATIONS**
7005 REM ****AVERAGE DEWPOINT READING****
7010 COLOR 3,1:LOCATE 21,5:PRINT"READING DEWPOINT 1234567890":COLOR
14,1
7020 RHV=0
7030 FOR I=1 TO 10
7040 L=LEN(CC$)
7050 CALL IOOUTPUTS (DEV,CC$,L)
7060 CALL IOENTER (DEV,DEWPOINT(I))
7070 CALL IOOUTPUTS(DEV,V1$,L)
7080 CALL IOENTER(DEV,HUM(I))
7090 CALL IOOUTPUTS(DEV,V2$,L)
7100 CALL IOENTER(DEV,RELH(I))
7110 D=D+DEWPOINT(I)
7120 RHV1=RHV1+HUM(I)
7130 RHV2=RHV2+RELH(I)
7140 COLOR 3,1:LOCATE 22,22+(I-1):PRINT"^":COLOR 14,1
7150 NEXT I
7160 REM **DD IS THE AVERAGE VOLTAGE OUTPUT FROM THE DEW
POINTER**
7170 DD=D/10#
7180 REM **DPT IS DD TRANSLATED INTO DEGREES C (2 DECIMAL
PLACES)**
7190 DPT=CINT(100#*(-40# + DD*20#))/100#
7200 RHV1=CINT(100#*RHV1*5#)/100#
7210 RHV2=CINT(100#*RHV2*2#)/100#
```

```
7220 LOCATE 21,36:PRINT"DEWPOINT: ";DPT
7230 LOCATE 21,53:PRINT"C"
7235 REM ****READING REFERENCE TEMPERATURE****
7236 REM ****READS T (VOLTS) OF THERMOCOUPLE IN CHANNEL OF RR$****
7240 L=LEN(RR$)
7250 CALL IOOUTPUTS (DEV,RR$,L)
7260 CALL IOENTER (DEV,VOLTR)
7265 REM ****READING DRY BULB TEMPERATURE****
7266 REM **READS T (VOLTS) OF THERMOCOUPLE IN CHANNEL OF TT$**
7270 L=LEN(TT$)
7280 CALL IOOUTPUTS (DEV,TT$,L)
7290 CALL IOENTER (DEV,VOLT5)
7295 REM ****CALCULATING REFERENCE TEMPERATURE****
7296 REM ****AND REFERENCE VOLTAGE****
7300 TR = VOLTR*10
7310 VREF=0
7320 IF TR<0 THEN GOSUB 3000
7330 IF TR>0 THEN GOSUB 3100
7340 V = VREF + ((VOLT5*1000#)*1000#)
7350 TEMP5=0
7360 IF V<0 THEN GOSUB 4000
7370 IF V>0 THEN GOSUB 4500
7380 PRINT"Tref:  ",TEMP5
7390 DT=SETT-TEMP5
7400 IF H< >2 THEN GOTO 7312
7410 OPEN "A:DATA.DAT" FOR APPEND AS #1
7420 PRINT #1,TEMP5,RH,RHV1,RHV2
7430 REM ****CALCULATING RELATIVE HUMIDITY (RH)****
7440 CLOSE #1
7450 H=H+1
7460 IF H=3 THEN H=0
7470 TEMP5=TEMP5*(1.0052#)+.1#
7480 T = DPT
7490 GOSUB 5000
7500 PSATDP=PSAT
7510 T = TEMP5
7520 GOSUB 5000
7530 PSATT5=PSAT
7535 REM ****RH IS THE RATIO OF THE SATURATED VAPOR PRESSURES
```

```
OF****
7536 REM ****THE DEWPOINT TO THE REFERENCE TEMPERATURE
(PERCENT)****
7540 RH=CINT(10000#*PSATDP/PSATT5)/100#
7550 LOCATE 6,5:PRINT"HUMIDITY: "; RH
7560 LOCATE 6,21:PRINT"%"
7570 LOCATE 7,5:PRINT"VAISALA1: "; RHV1
7580 LOCATE 7,21:PRINT"%"
7590 LOCATE 8,5:PRINT"VAISALA2: ";RHV2
7600 LOCATE 8,21:PRINT"%"
7610 RETURN
7999 REM **END READINGS AND CALCULATIONS**
8000 REM **BEGIN PROPORTIONAL-INTEGRAL-DERIVATIVE CONTROL**
8010 IF ABS(E)<.3 THEN IE=E+IE
8020 IF ABS(IE*E)<>(IE*E) THEN IE=0
8030 DE=E-E1
8040 E1=E
8050 NS=N*CINT(K*E - (K/TI)*IE + (K*TD)*DE)
8060 IF NS<0 THEN DIR=1 ELSE DIR=0
8070 NS=ABS(NS)
8080 IF ABS(DT)<.1 THEN IT=DT+IT
8090 DDT=DT-TP
8100 TP=DT
8110 C=C+CINT(TK*DT-(K/TI)*IT+(2#*K*TD)*DDT)
8120 IF C<2000 THEN C=2000
8130 IF C>2800 THEN C=2800
8140 D$=STR$(C)
8150 L=LEN(D$)-1
8160 C$=RIGHT$(D$,L)
8170 CALL IOOUTPUTS(DEV2,C$,L)
8180 RETURN
8999 REM **END PROPORTIONAL-INTEGRAL-DERIVATIVE CONTROL**
9000 REM **BEGIN INITIAL MOVEMENT**
9010 IF E=0 THEN 9070
9020 IF ABS(E)=E THEN GOSUB 10000 ELSE GOSUB 10100
9030 IF ABS(E)=E THEN N=1 ELSE N=-1
9040 NS=1
9050 E1=E
9060 DIR=0
9070 TP=DT
```

```
9080 GOSUB 6000
9090 RETURN
9999 REM **END INITIAL MOVEMENT**
10000 REM **BEGIN SOLENOID CONTROL**
10010 REM ****SWITCH SOLENOID TO DESSICANT****
10020 S$=SPACE$(25)
10030 S$="DO4,2"
10040 L=LEN(S$)
10050 CALL IOCLEAR(DEV)
10060 CALL IOOUTPUTS(DEV,S$,L)
10070 RETURN
10100 REM ****SWITCH SOLENOID TO BUBBLE****
10110 S$=SPACE$(25)
10120 S$="DC4,2"
10130 L=LEN(S$)
10140 CALL IOCLEAR(DEV)
10150 CALL IOOUTPUTS(DEV,S$,L)
10160 RETURN
10999 REM **END SOLENOID CONTROL**
```

APPENDIX C

Adsorption to desorption (A/D) ratios are useful in determining the amount of hysteresis in sorption isotherms. This ratio can be used in combination with direct sorption data to give a much clearer picture of the nature of moisture sorption. As stated earlier, the consensus between researchers appears to be that this ratio will fall between 0.7 and 0.9 for the sorption isotherms of most types of wood. The current data agree with this range in nearly all cases, as shown in Tables C-1 through C-3.

Table C-1. A/D ratios for the 25 C sorption isotherms.

RH (%)	EGS 1	EGS 2	OSB 1	OSB 2	FBS 1	FBS 2
10	0.81	0.84	0.82	0.82	0.83	0.83
20	0.83	0.83	0.83	0.83	0.83	0.83
30	0.83	0.83	0.82	0.80	0.83	0.83
40	0.84	0.83	0.85	0.85	0.83	0.83
50	0.82	0.82	0.83	0.82	0.84	0.84
60	0.85	0.85	0.83	0.83	0.81	0.82
70	0.85	0.85	0.83	0.84	0.83	0.83
80	0.85	0.83	0.84	0.83	0.84	0.83
90	0.85	0.85	0.86	0.86	0.82	0.83

Table C-2. A/D ratios for the 12 C sorption isotherms.

RH (%)	EGS 1	EGS 2	OSB 1	OSB 2	FBS 1	FBS 2
10	0.72	0.72	0.81	0.81	0.86	0.89
20	0.77	0.78	0.85	0.88	0.87	0.87
30	0.81	0.82	0.81	0.83	0.86	0.88
40	0.82	0.82	0.81	0.80	0.85	0.84
50	0.81	0.81	0.84	0.84	0.83	0.82
60	0.83	0.83	0.82	0.82	0.83	0.82
70	0.84	0.84	0.84	0.85	0.85	0.85
80	0.83	0.83	0.85	0.86	0.85	0.85

Table C-3. A/D ratios for the 55 C sorption isotherms.

RH (%)	EGS 1	EGS 2	OSB 1	OSB 2	FBS 1	FBS 2
10	0.77	0.80	0.77	0.77	0.95	0.95
20	0.78	0.80	0.78	0.76	0.97	0.94
30	0.76	0.76	0.77	0.78	0.95	0.93
40	0.76	0.75	0.77	0.77	0.96	0.95

APPENDIX D

Pederson (1990) proposed an equation for the prediction of scanning curves given the adsorption and desorption curves of a material. Since there is no reported physical basis for the value of the constant in the equation (0.1), an attempt was made to change its value so it better fits the exisiting scanning results from Peters (1992), Peralta (1995a), and the current experiment. In order to implement this equation, the adsorption and desorption isotherms of the materials tested in these three experiments were approximated using the Hailwood-Horrobin sorption model (Okoh and Skaar, 1980), which is of the form:

$$\gamma\ (\phi) = \frac{a_1\phi}{(1 + a_2\phi)(1 - a_3\phi)}$$

Pederson's approximation was revised by replacing the constant with various values, and comparing the resulting scanning curves with the existing scanning results. The constant only has a significant effect upon the beginning of the scanning curve, so it was chosen to match the first measured point of each scanning curve. These calculations showed that a constant of 0.75 is much more effective in correlating experimental data.

The improvement can be seen in Tables D-1 through D-4.

Table D-1. Comparison of Pederson's approximation and its revised form with the current desorption-to-adsorption scanning data.

RH	EGS 0.10	EGS 0.75	EGS Exp	OSB 0.10	OSB 0.75	OSB Exp	FBS 0.10	FBS 0.75	FBS Exp
50	8.1	8.1	8.1	7.6	7.6	7.6	7.5	7.5	7.5
40	7.8	7.2	7.2	7.3	6.8	6.6	7.2	6.8	6.7
30	6.8	6.5	6.2	6.2	6.1	5.6	6.1	6.0	5.7
20	5.2	5.2	5.0	4.7	4.7	4.4	4.7	4.7	4.6
10	3.2	3.2	3.1	2.8	2.8	2.7	2.9	2.9	2.8

Table D-2. Comparison of Pederson's approximation and its revised form with the current adsorption-to-desorption scanning data.

RH	EGS 0.10	EGS 0.75	EGS Exp	OSB 0.10	OSB 0.75	OSB Exp	FBS 0.10	FBS 0.75	FBS Exp
50	10.0	10.0	10.0	9.2	9.2	9.2	8.9	8.9	8.9
60	10.3	11.1	10.9	9.6	10.2	10.2	9.3	9.8	9.7
70	11.5	12.0	12.2	11.0	11.2	11.5	10.6	10.8	11.0
80	13.7	13.8	13.9	13.3	13.3	13.2	12.8	12.8	12.6
90	17.0	17.0	17.1	16.6	16.6	16.8	15.8	15.8	15.9

Table D-3. Comparison of Peterson's approximation and its revised form with Peters' data.

RH	EGS 0.10	EGS 0.75	EGS Exp	SuPin 0.10	SuPin 0.75	SuPin Exp	SoPin 0.10	SoPin 0.75	SoPin Exp
85	18.3	18.3	18.3	19.3	19.3	19.3	15.3	15.3	15.3
75	17.0	15.8	15.8	18.1	16.9	16.8	14.5	13.3	13.4
65	14.2	13.9	13.8	15.1	14.9	14.5	12.4	12.0	11.8
55	11.9	11.8	11.9	12.6	12.5	12.5	10.4	10.3	10.3
50	10.9	10.9	11.1	11.5	11.5	11.6	9.6	9.5	9.6

Table D-4. Comparison of Pederson's approximation and its revised form with Peralta's data.

RH	YelP 0.10	YelP 0.75	YelP Exp	YelP 0.10	YelP 0.75	YelP Exp	YelP 0.10	YelP 0.75	YelP Exp
92	20.91	20.91	20.91	x	x	x	x	x	x
75	14.77	14.71	14.46	12.44	12.44	12.44	x	x	x
53	10.18	10.18	10.11	9.99	9.38	9.73	8.27	8.27	8.27
32	6.67	6.67	6.62	6.67	6.66	6.50	6.63	6.33	6.17
11	3.20	3.20	3.16	3.20	3.20	3.11	3.20	3.20	3.06

VITA

The author, Joseph Richard Edwards, was born in Buffalo, New York on November 28, 1971. After spending his early childhood in Spring Lake Heights, New Jersey, he moved to northern Virginia, where he has lived since.

He received his bachelor's degree in mechanical engineering from Virginia Polytechnic Institute and State University in Blacksburg, Virginia in December 1993. After one semester spent in Blacksburg working as a tutor for the Virginia Tech Athletic Department, he began his graduate work.

After examining the current job market more thoroughly, he will decide whether to begin his working career or attend the Pennsylvania State University in pursuit of a doctoral degree in Acoustics.